Charles University in Prague

Faculty of Science

Study programme: Biochemistry

Study branch: Biochemistry

Inhibitors of mouse serine racemase

Inhibitory myší serinracemasy

Bc. Barbora Vorlová

Diploma Thesis

Supervisor: doc. RNDr. Jan Konvalinka, CSc.

Prague 2013

Prohlášení:

Prohlašuji, že jsem závěrečnou práci zpracovala samostatně a že jsem uvedla všechny použité informační zdroje a literaturu. Tato práce ani její podstatná část nebyla předložena k získání jiného nebo stejného akademického titulu.

V Praze dne ……

……

Barbora Vorlová

ACKNOWLEDGEMENTS

First of all, I would like to thank Jan Konvalinka for accepting me as a member of his research group and giving me a great deal of very valuable advice. I am very grateful for his professional as well personal support and for his conviction that I can do well in science.

Jana Jirásková and Hillary Hoffman also have my huge gratitude since they introduced me to the world of serine racemase and encouraged me not to give up even when nothing was going as expected.

I would like to thank Radko Souček for many kinetics measurements, Petr Jansa, Jiří Schimer and the research group of prof. Carlo De Micheli for preparation of most of the compounds for inhibitor screening and Klára Grantz Šašková for voluntary proof-reading of this thesis.

Huge thanks belong to all colleagues from 'Proteases of human pathogens' team who made the best working environment one can dream of. The combination of enjoyable research with many rewarding conversations over lunches and coffee breaks made me look forward to each day I spent there.

Last but not least, I would like to thank my parents for both moral and financial support and to all my friends for making my University years unforgettable. Special thanks belong to my lovely flatmates and dearest friends Diana Vondrušková, Zuzana Kofroňová and Lucie Berková for amazing six years spent in a pink apartment in the centre of Prague, Dáša Fastová who went through all difficulties of University life with me and cheered me up each time I needed it and Petra Fousová who made me sit down and write this thesis up.

ABSTRACT

Serine racemase (SR) is a pyridoxal-5'-phosphate-dependent enzyme responsible for biosynthesis of D-serine, a recognized neurotransmitter acting as a co-activator of N-methyl-D-aspartate (NMDA) type of glutamate receptors in the mammalian central nervous system. The hyperfunction of the mentioned receptors have been shown to be implicated in many neuropathological conditions including Alzheimer's disease, amyotrophic lateral sclerosis and epilepsy. To alleviate the symptoms of these diseases, several artificial blockers of NMDA receptors have been introduced into the clinical practice. However, many of these compounds cause undesirable side effects and it is thus necessary to search for either less harmful blockers or regulators of other targets of pharmaceutical intervention that are involved in NMDA receptor activation. In this context, specific inhibition of serine racemase seems to be a promising strategy for regulation of NMDA receptor overstimulation.

Mouse serine racemase shares 89% identity with its human ortholog and it was also shown that both enzymes possess similar kinetic parameters and inhibitor specificity. Therefore, the mouse models can be used to search for a potent human serine racemase inhibitor. Although many different compounds for their inhibitory potency towards serine racemase have been tested, no inhibitor with high binding affinity has been identified. This study aimed to build on the research performed so far and investigate whether the modifications of the most potent inhibitors of serine racemase published to date – L-*erythro*-3-hydroxyaspartate and malonate – could lead to increase of inhibitory efficiency towards the enzyme.

For this purpose, mouse serine racemase was expressed, purified and characterized. Subsequently, 50 compounds were tested for their inhibitory potency towards prepared enzyme and binding affinity and mechanism of action of the most efficient inhibitors was explored. This led to discovery of dichloromalonate as the compound with the highest binding affinity towards mouse serine racemase observed to date. Additionally, 3-hydroxyglutamates were identified as novel substrates of serine racemase side reaction activity possessing one of the best kinetic constants published to date.

Key words: serine racemase, inhibitor, substrate, pyridoxal phosphate, enzyme kinetics, inhibition mechanism

ABSTRAKT

Serinracemasa je pyridoxal-5'-fosfát dependentní enzym zodpovědný za biosyntézu D-serinu v centrální nervové soustavě. D-serin je důležitý neurotrasmiter, který se podílí na aktivaci N-methyl-D-aspartátových receptorů pro glutamát. Nadměrná stimulace zmíněných receptorů může vést k různým neuropatologiím, jako je Alzheimerova choroba, amyotropní laterální skleróza, epilepsie a další. Pro zmírnění příznaků těchto onemocnění se v klinické praxi využívají přímé blokátory NMDA receptorů. Řada těchto látek ale způsobuje nežádoucí účinky a je tedy zapotřebí hledat méně škodlivé blokátory či regulátory působící na jiné cíle terapeutického zásahu, které přímo ovlivňují aktivaci NMDA receptorů. V této souvislosti se právě specifická inhibice serinracemasy zdá být slibnou strategií pro snížení nadměrné stimulace dotyčných receptorů.

Myší serinracemasa sdílí 89% identitu se svým lidským ortologem, přičemž bylo prokázáno, že oba zmíněné enzymy vykazují podobné kinetické parametry a jsou inhibovány stejnými látkami s podobnou efektivitou. Pro hledání potentních inhibitorů lidské serinracemasy tedy mohou být využity myší modely. Nicméně, i přesto, že byla testována celá řada nejrůznějších látek, vysoce efektivní inhibitory serinracemasy ještě nebyly identifikovány. Tato studie měla za cíl navázat na výzkum provedený doposud a prozkoumat, zda modifikace zatím nejúčinnějších publikovaných inhibitorů serinracemasy – L-*erythro*-3-hydroxyaspartátu a malonátu – může vést k zisku více potentních regulátorů dotyčného enzymu.

Za tímto účelem byla exprimována, purifikována a charakterizována myší serinracemasa. 50 různých sloučenin bylo následně testováno pro jejich potenciální inhibiční aktivitu vůči připravenému rekombinantnímu enzymu. U nejúčinnějších látek byla poté prozkoumávána vazebná afinita a mechanismus inhibice, přičemž byl nalezen doposud nejefektivnější kompetitivní inhibitor serinracemasy – dichloromalonát. Zároveň byly identifikovány nové substráty vedlejší reakční aktivity serinracemasy, které vykazují jedny z nejlepších dosud publikovaných kinetických konstant.

Klíčová slova: serinracemasa, inhibitor, substrát, pyridoxalfosfát, enzymová kinetika, mechanismus inhibice

TABLE OF CONTENTS

1. INTRODUCTION 1

1.1. DISCOVERY OF SERINE RACEMASE 1

1.2. FUNCTION AND METABOLISM OF D-SERINE 2

1.2.1. D-serine as the neurotransmitter in the central nervous system 2
1.2.1.1. Activation of NMDA receptors by D-serine 2
1.2.1.2. Roles of D-serine resulting from NMDA receptor activation 4
1.2.2. Other physiological functions of D-serine 4
1.2.3. D-serine metabolism 5
1.2.3.1. Biosynthesis of D-serine 5
1.2.3.2. Degradation of D-serine 5

1.3. BIOLOGY AND PATHOBIOLOGY OF SERINE RACEMASE 7

1.3.1. Serine racemase orthologs within mammals 7
1.3.2. Localization of serine racemase 7
1.3.3. Physiological function of serine racemase 8
1.3.4. Serine racemase in neuropathology 9

1.4. BIOCHEMISTRY OF SERINE RACEMASE 10

1.4.1. Serine racemase enzyme activities 10
1.4.1.1. Kinetic parameters of reactions catalyzed by serine racemase 11
1.4.1.2. Other substrates of SR 12
1.4.2. Serine racemase activators 13
1.4.3. Posttranslational modifications and interaction partners of serine racemase 14
1.4.4. Serine racemase structure 15
1.4.5. Inhibitors of serine racemase 17

2. AIMS AND OBJECTIVES 21

3. MATERIALS AND METHODS 22

3.1. MATERIALS 22

3.1.1. Chemicals 22
3.1.2. Compounds for inhibition testing 24
3.1.3. Instruments 29
3.1.4. Other material 30

3.2. METHODS 32

3.2.1. Mouse serine racemase expression 32
3.2.2. mSR purification 33
3.2.2.1. Cell lysis 33
3.2.2.2. Ammonium sulfate precipitation 33
3.2.2.3. Reversed-phase chromatography 33
3.2.2.4. Ion-exchange chromatography 34
3.2.2.5. Affinity chromatography 34
3.2.3. Assessment of mSR purity and enzymatic activity 34
3.2.3.1. Determination of protein concentration 34
3.2.3.2. Sodium dodecyl sulfate-polyacrylamide gel electrophoresis (SDS-PAGE) 35
3.2.3.3. Commassie Briliant Blue staining of polyacrylamide gel 36
3.2.3.4. Western blotting using semi-dry transfer 36
3.2.3.5. Determination of specific activity of mSR 36
3.2.3.6. Measurements of kinetics of L-serine racemisation 38
3.2.3.7. Determination of kinetic constants for L-serine racemisation 38
3.2.4. Testing of compounds for their inhibitory efficiency towards mSR 39
3.2.4.1. Preparation of the compound solutions 39

3.2.4.2. Inhibition analysis 39
3.2.4.3. Result processing 40
3.2.5. Enzymatic measurements with novel mSR substrates *41*
3.2.5.1. Testing of compounds as possible substrates of mSR 41
3.2.5.2. Determination of kinetic constants for novel substrates of mSR 41

4. RESULTS 43

4.1. PREPARATION AND KINETIC CHARACTERIZATION OF RECOMBINANT MSR 43

4.1.1. mSR preparation *43*
4.1.2. Kinetic characterization of the recombinant mSR *45*

4.2. INHIBITION STUDIES ON MSR 46

4.2.1. Malonate-based compounds *47*
4.2.2. Hydroxyglutamates and their derivatives *51*
4.2.3. Miscellaneous compounds *53*

4.3. NOVEL SUBSTRATES OF MSR 54

5. DISCUSSION 58

6. CONCLUSIONS 63

7. ABBREVIATIONS 64

8. REFERENCES 66

1. INTRODUCTION

1.1. Discovery of serine racemase

For most of the history of biochemistry, L-amino acids have been known to be essential for all living organisms, while their D-enantiomers have been considered to be crucial only for bacteria [1]. Even when in 1965, D-alanine was detected in body fluids of guinea pigs and mice in metabolically significant quantities [2], it was not believed that this amino acid fulfils any physiological function in higher organisms. Moreover, D-amino acids were not generally assumed to be formed in mammals *de novo*. They were suggested to originate from exogenous sources such as diet, intestinal microflora and spontaneous racemisation of L-amino acids after protein hydrolysis [1].

In the following 30 years, high levels of D-aspartate [3-5] and D-serine [6-7] were identified in brain of rodents and humans. Furthermore, the concentration of D-serine in the central nervous system (CNS) of mature rats appeared to be higher than the amount of any other D-amino acid determined in mammalian brain ever before [6]. Together with the fact that 4 years prior its first detection in mammals, D-serine was observed to be capable of activation of excitatory N-methyl-D-aspartate (NMDA) receptors [8], the discovery of D-enantiomer of serine in mammalian CNS seemed to be very important. It was proposed that D-serine could be a novel endogenous neurotransmitter [6].

However, the origin of this amino acid was uncertain. Indeed, based on the study performed previously by Oldendorf, free D-serine could have not been derived from diet since it was believed that the transport of serine through the blood-brain barrier is very slow [9]. It was thus desirable to search for the mechanism of D-serine formation in the brain. In 1997, L-serine was proposed to be the possible source of D-serine and it was suggested that the racemisation reaction is catalyzed by a specific racemase [10-11]. This hypothesis was finally confirmed two years later, when Wolosker and co-workers published a study revealing the characterization of rat serine racemase (rSR), an enzyme capable of converting L-serine to its D-enantiomer [12].

1.2. Function and metabolism of D-serine

1.2.1. D-serine as the neurotransmitter in the central nervous system

As mentioned above, the participation of D-serine in neurotransmission in the mammalian brain was first suggested in early 1990s [6,13]. Since then, many studies have been conducted to confirm the proposed function of D-serine and investigate the physiological role of this amino acid further [13-15]. Currently, D-serine is widely recognized as the co-agonist of N-methyl-D-aspartate type of glutamate receptors, the receptors involved in neuronal development, synaptic plasticity, learning, memory and neurotoxicity [16].

1.2.1.1. Activation of NMDA receptors by D-serine

N-methyl-D-aspartate (NMDA) receptors are tetrameric ligand-gated ion channels participating in glutamatergic excitatory neurotransmission [17]. They are formed by a combination of two distinct subunits (NR1 and NR2) that bear specific binding sites for several factors influencing the signal transmission (see Figure 1, p. 3) [18-19]. NMDA receptors are permeable to three different ions – potassium, sodium and calcium. To enable the ions to penetrate through the channel, the receptor needs to first be stimulated. This is carried out by glutamate as an agonist that binds to the glutamate site on the NR2 subunit and glycine or D-serine as a co-agonist that binds to the glycine site on the NR1 subunit [18,20-21]. Occupancy of both sites is required to achieve complete activation of the NMDA receptors.

Since both glycine and D-serine have been suggested to act as neurotransmitters by binding to the glycine site of NMDA receptors, it has been desirable to investigate whether both compounds are equally important for the successful transmission of the signal through the channels. Based on the first experiments, it was proposed that each of the compounds could probably serve as the main co-activator of NMDA receptors depending on the brain region [17]. However, most recent reports prioritize D-serine, rather than glycine, as the major co-agonist of these receptors [14].

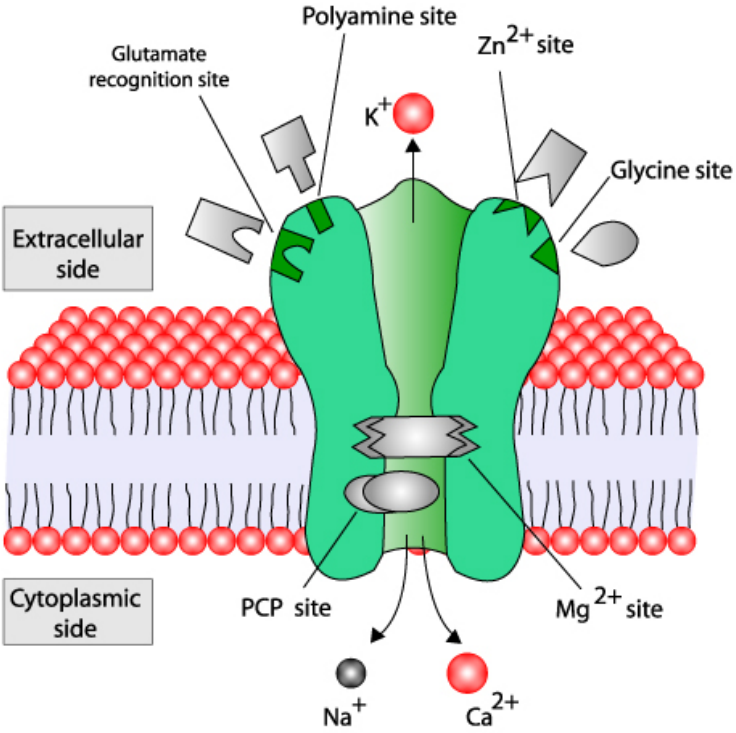

Figure 1: Schematic representation of NMDA receptor. NMDA receptors are ion channels permeable to potassium, sodium and calcium. In order to open, both glutamate recognition site and so-called glycine site need to be occupied. Moreover, magnesium ion bound inside of the channel needs to be released. The function of NMDA receptors is stimulated by binding of specific polyamines and inhibited by zinc and phencyclidines (PCP) [18-19]. The figure was adapted from [22].

Indeed, several studies have revealed that the localization of NMDA receptors in the brain corresponds with the localization of D-serine more precisely than with glycine [23-24]. Moreover, in comparison with glycine, D-serine appeared to have higher affinity as well as potentiation effectivity towards NMDA receptors [25-27].

Most of the reports dealing with the establishment of major endogenous co-agonist of NMDA receptors focused on the observation of the responses of these receptors in the absence of D-serine (Fuchs 2011). It was shown that enzymatic depletion of D-serine from different types of brain slices, primary cell cultures and vertebrate retina leads to dramatic decrease of NMDA receptor activity [28-33]. Furthermore, knock-out of the D-serine synthesizing enzyme (serine racemase) gene in mice resulted in the reduction of NMDA receptor functions as displayed by learning and memory impairments [34]. It is thus undoubtable that D-serine plays an important role in NMDA receptor neurotransmission.

1.2.1.2. Roles of D-serine resulting from NMDA receptor activation

NMDA receptors fulfil wide variety of functions in the CNS (see charter 1.2.1). Since D-serine is accepted as their co-activator, it is not surprising that this amino acid appears to play a key role in some of the physiological processes linked with these receptors. To date, D-serine has been confirmed to participate in neuronal development [35] and long term potentiation (LTP) which is considered to be one of the molecular mechanisms of learning and memory [36].

As well as being crucial for higher organisms in physiological conditions, NMDA receptors could participate in many neuropathologies including brain ischemia, epilepsy, schizophrenia and neurodegenerative disorders [17,37]. From those, the role of D-serine has been reported to be implicated in epilepsy, schizophrenia, perinatal asphyxia, amyotrophic lateral sclerosis (ALS), Alzheimer's disease and bipolar disorder [14,38-39].

1.2.2. Other physiological functions of D-serine

Apart from the brain, D-serine has been detected in blood [40], saliva [41], urine [42] and retina [29], revealing that this amino acid can occur in peripheral mammalian tissues [38]. However, whether the presence of D-serine outside of the CNS is physiologically significant still remains to be elucidated.

Recently, D-serine has been proposed to be involved in lower esophageal sphincter contraction and peripheral nerve relaxation through modulation of NMDA receptors [43-44]. In addition, this amino acid has also been shown to negatively regulate chondrogenesis and osteoclastogenesis [45-46].

1.2.3. D-serine metabolism

1.2.3.1. Biosynthesis of D-serine

The main synthesizing enzyme of D-serine in mammalian CNS is serine racemase [12] (for more details see Chapter 1.4.1). Nevertheless, several studies have shown that the depletion of D-serine in serine racemase knock-out mice is not complete [34] suggesting that there must be an alternative way of D-serine acquisition. One such an income could be from exogenous sources (see Chapter 1.1). Indeed, contrary to preliminary observations by Oldedorf (see Chapter 1.1), more recent research has revealed that D-serine can be easily transported from blood to the brain through the blood brain barrier [47]. In addition, the possible involvement of the glycine cleavage system and phosphoserine phosphatase in D-serine biosynthesis has also been investigated [48-49].

The glycine cleavage system (GCS) is a series of enzymes that participate in catabolism of glycine [50]. The main glycine degradation products in this pathway are carbon dioxide and ammonia. However, it was also proposed that glycine might be converted into D-serine [48]. It is not clear though, whether this reaction is catalyzed only by GCS or other enzymes such as serinhydroxymethyltransferase are also required.

Using phosphoserine phosphatase, it has been suggested that D-serine may be synthesized from D-phosposerine [49]. Nevertheless, since D-phosposerine has not been detected in mammals [51] this source of D-serine seems to be unlikely.

1.2.3.2. Degradation of D-serine

Similarly to D-serine biosynthesis, D-serine catabolism is also not yet fully understood. However, it is believed that the major role in degradation of this amino acid plays D-amino acid oxidase (DAAO) [52]. This flavine-adenine dinucleotide (FAD) enzyme is not specific only for D-serine but generally catalyzes oxidative deamination of D-amino acids into iminoacids with the concurrent release of H_2O_2 [53]. In the case of D-serine, this leads to a generation of imino pyruvic acid which is subsequently non-enzymatically hydrolyzed to pyruvate and ammonia (see Figure 2, p. 6) [54].

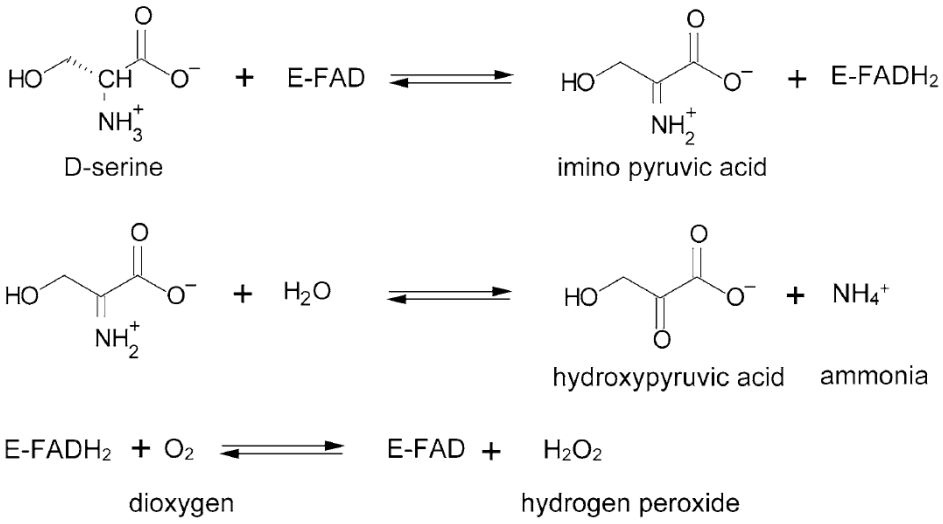

Figure 2: Degradation of D-serine catalyzed by FAD-dependent D-amino acid oxidase. The α-proton is first transferred from D-serine to oxidised FAD to form imino pyruvic acid and reduced flavin. The imino pyruvic acid is subsequently non-enzymatically converted into pyruvate and ammonia while $FADH_2$ is re-oxidized by dioxygen into FAD with simultaneous production of hydrogen peroxide. The scheme was taken from [54].

The hypothesis that DAAO is a key player in D-serine degradation has been confirmed by several independent studies using mutant mice lacking DAAO activity [55]. Indeed, the overall amount of D-serine in the brains of genetically modified mice was much higher than in the brains of normal mice. However, in some brain regions of mutant mice, the concentration of D-serine remained unchanged. It could not be thus excluded that other enzymes than DAAO participate in D-serine catabolism in these areas of the CNS [15]. In this context, serine racemase (SR) has been suggested as one such a candidate since in addition to its racemisation activity, this enzyme is able to eliminate D-serine to pyruvate *in vitro* [56] (for more details see Chapter 1.4.1). Nevertheless, it has not yet been investigated whether the elimination activity of SR is involved in D-serine degradation *in vivo*.

1.3. Biology and pathobiology of serine racemase

1.3.1. Serine racemase orthologs within mammals

To date, three different mammalian serine racemase orthologs have been identified and studied – rat SR (rSR), mouse SR (mSR) and human SR (hSR) [57]. While the preliminary experiments were conducted on rats, recent research dealing with the biology, pathobiology and biochemistry of serine racemase is more focused on mice and humans. The primary structures of all mentioned SRs are very similar since the sequence alignment among hSR, mSR and rSR revealed 90% identity [57].

In addition, the gene sequence of serine racemases from cow, dog, chimpanzee and rhesus monkey have been deposited in databases. However, almost no experimental data are yet available for these mammalian SR orthologs [58].

1.3.2. Localization of serine racemase

The current expressed sequence tag (EST) profile available in the NCBI Unigene database suggests that human SR mRNA could occur in brain, kidney, liver, skeletal muscle, heart, intestine, lung, thymus, adrenal gland, bone, eye, mammary gland, pharynx, prostate, stomach, testis and uterus [59]. Northern blot performed by Xia and colleagues confirmed the presence of SR mRNA in human brain, liver, kidney, muscles and heart. On the other hand, no signal was observed in intestine, lung and thymus [60]. These results corresponded with those previously obtained with mice [61].

On the protein level, SR has been shown to be expressed in human brain, kidney and heart [60]. Additionally, the experiments with rodents revealed the presence of SR protein in liver [61], peripheral nervous system [62], retina [29,63] and peripheral vestibular system [64].

Within the brain, SR is localized most likely in both neurons and glial cells [58]. In fact, the cellular distribution of this enzyme is slightly controversial. The first report suggested SR to be an astrocytic enzyme [65]. However, in subsequent studies, SR was observed to be present in neurons as well as glia [31,66-67] and one publication even indicated SR to

be more abundant in neurons [68]. Moreover, a complete absence of SR in glial cells has been also already reported [69].

Within the cell, SR was shown to be predominantly localized in cytosol [58]. Nevertheless, a small fraction of SR could be also bound to the membrane through the acylated residues (see Chapter 1.4.3) [70].

1.3.3. Physiological function of serine racemase

Since SR serves as the main biosynthetic enzyme of D-serine it is not surprising that the physiological function of this enzyme closely corresponds with the role of NMDA receptors (see Chapter 1.2.1). The involvement of SR in NMDA receptor neurotransmission has been already demonstrated by several SR knock-out mice studies.

The deletion of SR gene results in significant reduction of NMDA receptor-mediated excitatory postsynaptic currents [71] and decreased propensity to neurotoxicity [72-73]. Moreover, SR knock-out mice display behavioural changes and defects in learning and memory that are usually connected with NMDA receptor hypofunction [34]. Indeed, targeted disruption of SR was shown to affect the memory for order [74], caused hyperactivity and impairment of spatial memory in males and elevation of anxiety in females [71].

While the importance of SR racemisation activity is apparent, the physiological significance of SR elimination activity is still a subject of speculations. The involvement of SR in energetic metabolism seems to be unlikely since the amount of pyruvate formed from serine represents less than 0.1% of the amount generated during glycolysis [75]. The only reasonable suggestion of the role of SR elimination activity is thus the involvement of this enzyme in D-serine degradation [56]. It cannot be also excluded that this activity is only a vestige of evolution and β-elimination is thus just a side reaction of SR [76].

1.3.4. Serine racemase in neuropathology

Similarly to the connection of SR physiological role with NMDA receptor functions, the pathophysiology of this enzyme closely corresponds with NMDA receptor dysfunction. To date, the possible involvement of SR has been suggested in neuropathology of schizophrenia, Alzheimer's disease, ALS and epilepsy.

In fact, the participation of SR in pathology of schizophrenia is still a matter of speculations since the results gained from studies addressing this topic are inconclusive and controversial [58]. It was observed that in comparison with age and sex-matched healthy controls, schizophrenics possess lower D-serine levels in serum and cerebrospinal fluid [77-78]. However, this phenomenon does not necessarily have to be connected with decrease of SR expression or activity and could easily be caused by up-regulation of DAAO, the D-serine degrading enzyme (see Chapter 1.2.3.2).

The relationship between SR and other mentioned diseases has been demonstrated more clearly. The levels of SR mRNA were shown to be increased in human brain samples of Alzheimer's disease patients when compared with age-matched controls [79]. Moreover, SR knock-out mice displayed significantly reduced propensity to neurotoxicity after administration of amyloid β-peptide (Aβ), an agent responsible for formation of so-called amyloid plaques in the brain of Alzheimer's disease patients.

SR up-regulation has been also observed in G93A-SOD1 transgenic mice, which is the standard model of ALS [80-81]. The progress of the disease is much slower in ALS mice with disrupted SR [81]. Additionally, the presence of phenazine methosulfate, an alleged SR inhibitor, in the media of primary cultured spinal cord cells from ALS mice leads to significant alleviation of NMDA toxicity [80].

Finally, increasing evidence suggests that SR plays a role in pathology of epilepsy. The enzyme was shown to be overexpressed in the experimental model of this disease [82] and furthermore, SR knock-out mice are much less susceptible to seizures induced by pentylenetrazole, an agent used to evoke experimental epilepsy, relative to wild-type mice [83].

1.4. Biochemistry of serine racemase

1.4.1. Serine racemase enzyme activities

Serine racemase was discovered as an enzyme responsible for conversion of L-serine to D-serine and *vice versa* (see Figure 3) [12]. Since the affinity of serine racemase towards L-serine is several times higher than towards D-serine [12,84-85] and furthermore the amount of L-serine in CNS is estimated up to 70 – 98% of total serine [86] it is believed that in the physiological conditions, SR preferably catalyzes the racemisation of L-serine to D-serine.

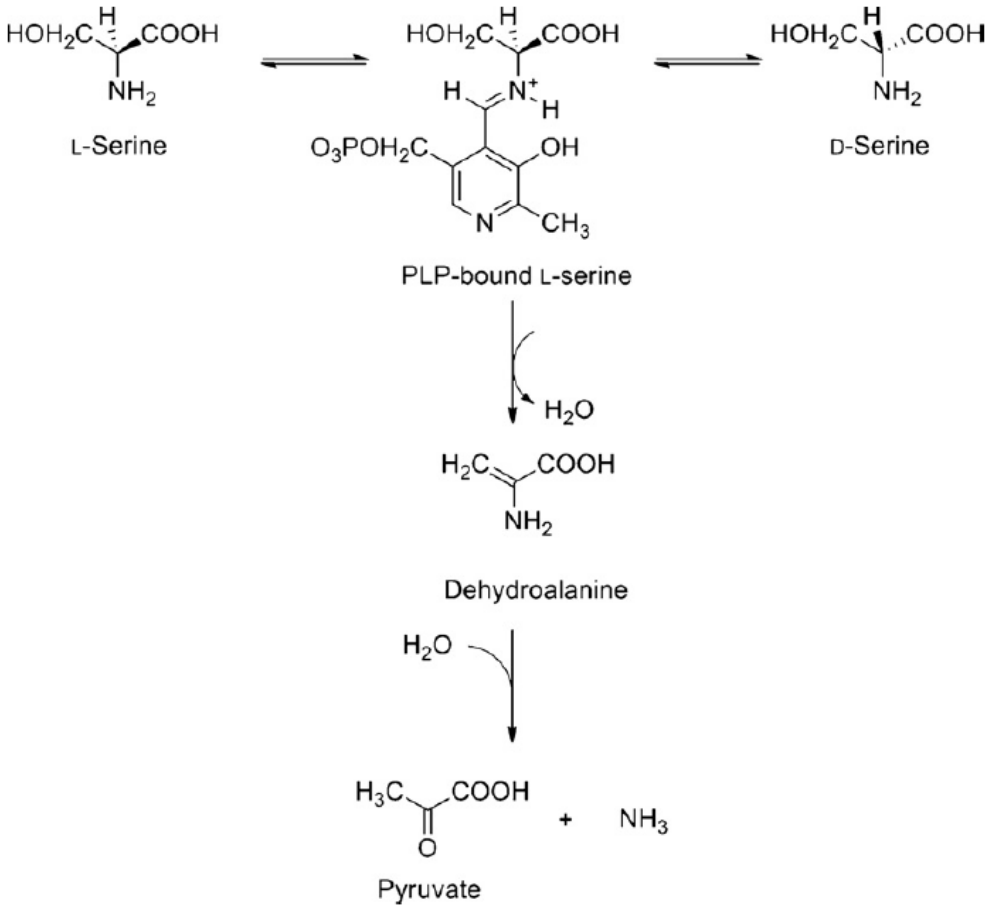

Figure 3: The reactions catalyzed by serine racemase. Serine racemase is capable of racemisation of L-serine as well as D-serine and elimination of water from both compounds to form dehydroalanine which is subsequently hydrolyzed into pyruvate and ammonia. Since serine racemase is PLP-dependent enzyme all mentioned reactions are carried over the condensation of PLP with the amino acid substrate to form a Schiff base. The scheme was taken from [16].

As already mentioned, in addition to its racemisation activity, SR also possesses β-elimination activity (see Figure 3, p. 10) [87-88]. Indeed, it was shown that both L-serine and D-serine are deaminated into pyruvate in the presence of SR. Both racemisation and elimination reactions share the same active site and require pyridoxal-5'-phosphate (PLP) as a cofactor (see Figure 3, p. 10). The optimum condition for the enzyme during these reactions is a pH in the alkaline range (pH 8.0 – 9.0) and a temperature of 37˚C.

The necessity of the presence of PLP in SR catalyzed reactions was observed from the very beginning [12]. Indeed, Wolosker and co-workers reported that the SR activity is inhibited when agents reacting with PLP are added into the enzymatic reaction. Moreover, the absorption spectrum of SR showed the same trend as the absorption spectra characteristic for PLP-dependent enzymes [12]. Subsequently, the determination of the mSR primary structure was published and revealed the presence of a conserved sequence for PLP-binding [65]. This sequence is usually located in the active site of the PLP-dependent enzyme and contains lysine through which the PLP can be covalently bound to the enzyme [57]. The lysine for PLP-binding to the active site of SR has been identified for both mSR and hSR as K53. However, several studies have pointed out that PLP is bound to SR weakly since the enzyme looses its activity when it is dialyzed against buffer without added PLP [58]. Despite of this discrepancy in a typical PLP-dependent enzyme behaviour, SR is considered as a member of the fold-type II family of PLP-dependent enzymes [58].

1.4.1.1. Kinetic parameters of reactions catalyzed by serine racemase

The kinetic parameters of SR differ depending on the species, the way of enzyme preparation and the reaction conditions used. K_m of L-serine ranges from 1.8 mM to 60 mM and k_{cat} ranges from 3 to 45 min^{-1} for SR racemisation and 7 to 115 min^{-1} for SR β-elimination [76]. While almost no kinetic data are available for rat SR, mouse SR enzyme parameters have been investigated extensively [89]. Moreover, recombinant human SR has been already prepared and compared with its recombinant mouse ortholog produced using the same *E.coli* expression system [85] (see Table 1, p. 12).

Table 1: Kinetic parameters of L- and D-serine racemisation and L- and D-serine *β*-elimination catalyzed by mouse and human serine racemase. Data taken from [85].

	mSR			hSR		
REACTION	K_m [mM]	k_{cat} [min^{-1}]	k_{cat}/K_m [$min^{-1}mM^{-1}$]	K_m [mM]	k_{cat} [min^{-1}]	k_{cat}/K_m [$min^{-1}mM^{-1}$]
L-serine racemisation	3.8 ± 0.1	45.5 ± 0.5	12.0 ± 0.4	4.1 ± 0.2	41.5 ± 1.5	10.0 ± 0.8
D-serine racemisation	14.5 ± 1.1	113 ± 3	7.8 ± 0.6	10.8 ± 0.8	84.9 ± 4.2	7.9 ± 0.9
L-serine *β*-elimination	4.0 ± 0.5	81.3 ± 2.8	20.3 ± 2.6	4.7 ± 0.4	100 ± 5.1	21.2 ± 2.7
D-serine *β*-elimination	3.2 ± 0.3	8.8 ± 0.2	2.7 ± 0.4	9.5 ± 0.6	7.7 ± 0.3	0.81 ± 0.09

The study revealed that both enzymes behave very similarly. The only difference was observed in deamination of D-serine. Indeed, it seems that in contrast with hSR, mSR is not able to convert D-serine to pyruvate directly. The kinetic data determined for D-serine elimination catalyzed by mSR rather correspond with the deamination of L-serine previously synthesized from D-serine by racemisation [85].

1.4.1.2. Other substrates of SR

The racemisation activity of SR has been shown to be highly specific to serine. The only exception represents threonine since L-*allo*-threonine can be converted to D-threonine and *vice versa* and D-*allo*-threonine can be converted to L-threonine and *vice versa* [84]. However, the affinity of the threonine isomers towards SR is very low and it is thus not believed that these reactions could be physiologically relevant.

Contrary to SR racemisation specificity, several different compounds have been reported to be substrates of SR during *β*-elimination [84] (for the list of the substrates see Tabel 2, p. 13). These include both naturally occurring and artificial amino acids and their derivatives which are deaminated into the corresponding oxo-acid products. Surprisingly, some of the compounds have much higher affinity towards SR than L-serine itself and moreover some elimination reactions are much faster than L-serine racemisation (compare

Table 1, p. 12 with Table 2). The best substrates of mSR published to date are L-serine-*O*-sulfate, L-*threo*-3-hydroxy-aspartate and *β*-chloro-L-alanine.

Table 2: Kinetic parameters of *β*-elimination of substrates other than serine catalyzed by mouse serine racemase. Data taken from [84].

SUBSTRATE	PRODUCT	K_m [mM]	k_{cat} [min^{-1}]	k_{cat}/K_m [$min^{-1}mM^{-1}$]
L-serine-*O*-sulfate	pyruvate	0.49 ± 0.05	967 ± 17	1973 ± 205
β-chloro-L-alanine	pyruvate	1.6 ± 0.4	155 ± 10	97 ± 13
L-*threo*-3-hydroxyaspartate	oxalacetate	1.0 ± 0.1	1860 ± 60	1788 ± 214
L-threonine	2-oxobutyrate	48 ± 5	627 ± 25	13.1 ± 1.5

From the compounds determined as the other substrates of SR during *β*-elimination (see Table 2), only L-threonine can be detected in mammals. Since this amino acid has very low affinity towards SR it is believed that the ability of SR to deaminate substrates other than serine is only a vestige of the evolution [76]. In fact, even in the case of serine, the physiological significance of SR *β*-elimination in mammals is still debated (see Chapter 1.3.3).

1.4.2. Serine racemase activators

As already mentioned, PLP is the crucial cofactor in reactions catalyzed by SR. In addition, several other activators and cofactors such as divalent cations, nucleotides and reducing agents have been shown to increase SR activity significantly.

Among divalent cations, Mg^{2+}, Mn^{2+} and Ca^{2+} are the most potent activators of SR [88,90]. In contrast, Fe^{2+} and Ni^{2+} have almost no effect and Cu^{2+}, Co^{2+}, and Zn^{2+} even inhibit SR activity [88]. The necessity of the presence of divalent cations in the enzymatic reaction has been demonstrated by rapid decrease of SR activity when chelators such as EDTA were added [90]. However, it is still speculated which of the mentioned ions is responsible for regulation of SR activity *in vivo* [58]. Despite the suggestion that Ca^{2+} as an abundant second messenger in the brain could play a role in SR stimulation, it is assumed that rather

Mg^{2+} is involved in this process since its concentration in neuronal cells exceeds the necessary amount several times [87].

The most potent activator of SR within nucleotides is ATP followed by less effective ADP, GTP, UTP and CTP. Surprisingly, ATP serves only as an allosteric regulator since it is not hydrolyzed into ADP and phosphate during the enzymatic reaction [87,91]. Moreover, it has been demonstrated that the effect of ATP is enhanced when 1,4-dithiothreitol (DTT) is present in the reaction [92-93]. Indeed, reducing agents such as DTT, triscarboxyethylphosphine (TCEP), reduced glutathione and mercaptoethanol have been shown to increase SR activity [92]. Since SR is predominantly localized in cytosol (see Chapter 1.3.2), which is known to be a reducing environment [94], and ATP and Mg^{2+} have additive activation effects on SR [87], it is believed that all these factors together determine the SR efficiency *in vivo* [57-58].

1.4.3. Posttranslational modifications and interaction partners of serine racemase

It is assumed that posttranslational modifications are not crucial for SR activity since kinetic parameters of recombinant serine racemase prepared using an *E.coli* expression system [84,90] are comparable with kinetic parametrs of serine racemase isolated from mouse brains [91]. However, several different posttranslational modifications have been reported to inactivate SR or participate in SR degradation.

Mustafa and co-workers suggested that mSR could be S-nitrosylated at C113 residue. This leads to inhibition of enzyme activity [93]. In addition, Balan and colleagues showed that SR undergoes acylation which mediates translocation of SR into the plasma membrane [70]. This process is probably involved in regulation of D-serine production since membrane-bound SR is much less efficient. Moreover, phosphorylation of T227 seems to be crucial for steady-state binding of mSR to the membrane [70]. This observation is particularly interesting since SR contains a number of potential phosphorylation sites [57] but no other phosphorylation has been reported to date. Finally, the study of Dumin and co-workers revealed that SR undergoes polyubiquitination prior its degradation through the ubiquitin-proteasomal system [95].

In contrast with posttranslational modifications of SR published so far, the SR interaction partners initially identified by yeast two-hybrid screening seem to increase the enzyme activity and prevent its degradation [96]. Indeed, binding of glutamate receptor interacting protein (GRIP) [97-98] and protein interacting with kinase C (PICK1) [99] to the C-terminus of mSR and hSR could lead to enzyme stimulation. Similarly, interaction of golgin subfamily A member 3 (Golga 3) with the N-terminus of SR has been shown to inhibit polyubiqutination of SR resulting in a significant increase in protein half-life [95].

1.4.4. Serine racemase structure

As mentioned above, the primary structures of the three studied mammalian SRs – hSR, mSR and rSR – are very similar (see Chapter 1.3.1). The sequence alignment of these SRs is depicted in Figure 4. hSR consists of 340 amino acids and its predicted molecular weight is 36.5 kDa. mSR is formed by 339 residues with a total size of 36.4 kDa. rSR is composed of 333 amino acids, giving it a molecular weight of 35.7 kDa. Interestingly, in comparison with mSR and hSR, rSR is truncated at the C-terminus, which leads to loss of sequence motif responsible for interaction of SR with GRIP and PICK1 (see Chapter 1.4.3).

```
hSR    MCAQYCISFADVEKAHINIRDSIHLTPVLTSSILNQLTGRNLFFKCELFQKTGSFKIRGA 60
mSR    MCAQYCISFADVEKAHINIQDSIHLTPVLTSSILNQIAGRNLFFKCELFQKTGSFKIRGA 60
rSR    MCAQYCISFADVEKAHLNIQDSVHLTPVLTSSILNQIAGRNLFFKCELFQKTGSFKIRGA 60
       ****************:**:**:*************::**********************

hSR    LNAVRSLVPDALERKPKAVVTHSSGNHGQALTYAAKLEGIPAYIVVPQTAPDCKKLAIQA 120
mSR    LNAIRGLIPDTPEEKPKAVVTHSSGNHGQALTYAAKLEGIPAYIVVPQTAPNCKKLAIQA 120
rSR    LNAIRGLIPDTLEGKPKAVVTHSSGNHGQALTYAAKLEGIPAYIVVPQTAPNCKKLAIQA 120
       ***:*.*:**: * ************************************:********

hSR    YGASIVYCEPSDESRENVAKRVTEETEGIMVHPNQEPAVIAGQGTIALEVLNQVPLVDAL 180
mSR    YGASIVYCDPSDESREKVTQRIMQETEGILVHPNQEPAVIAGQGTIALEVLNQVPLVDAL 180
rSR    YGASIVYSEPSDESRENVAQRIIQETEGILVHPNQEPAVIAGQGTIALEVLNQVPLVDAL 180
       *******.:*******:*::*: :*****:******************************

hSR    VVPVGGGGMLAGIAITVKALKPSVKVYAAEPSNADDCYQSKLKGKLMPNLYPPETIADGV 240
mSR    VVPVGGGGMVAGIAITIKALKPSVKVYAAEPSNADDCYQSKLKGELTPNLHPPETIADGV 240
rSR    VVPVGGGGMVAGIAITIKTLKPSVKVYAAEPSNADDCYQSKLKGELTPNLHPPETIADGV 240
       *********:******:*:*************************:* ***:*********

hSR    KSSIGLNTWPIIRDLVDDIFTVTEDEIKCATQLVWERMKLLIEPTAGVGVAAVLSQHFQT 300
mSR    KSSIGLNTWPIIRDLVDDVFTVTEDEIKYATQLVWGRMKLLIEPTAGVALAAVLSQHFQT 300
rSR    KSSIGLNTWPIIRDLVDDVFTVTEDEIKYATQLVWERMKLLIEPTAGVGLAAVLSQHFQT 300
       ******************:********* ****** ************.:**********

hSR    VSPEVKNICIVLSGGNVDLTSSITWVKQAERPASYQSVSV 340
mSR    VSPEVKNVCIVLSGGNVDLTS-LNWVGQAERPAPYQTVSV 339
rSR    VSPEVKNICIVLSGGNVDLTS-LSWVKQAERPAP------ 333
       *******:************* :.** ******.
```

Figure 4: Comparison of primary structures of human, mouse and rat serine racemase. The asterisks indicate positions with fully conserved residues, the colons highlight conservation between groups of strongly similar properties identical residues and the dots mark conservation between groups of weakly similar properties. Sequence alignment was generated by ClustalW2 [100].

Secondary structure of recombinant mSR and hSR has been predicted using circular dichroism spectroscopy [85]. The study revealed that hSR contains 40.3% α-helixes, 6.9% antiparallel β-sheets, 7.0% parallel β-sheets, 15.8% β-turns, and 27.1% random coils. Similarly, the composition of mSR secondary structure is as follows: 43.9% α-helix, 6.5% antiparallel β-sheet, 6.3% parallel β-sheet, 15.4% β-turn, and 24.3% random coil [85].

The three-dimensional structure of mammalian SRs from X-ray data is available for hSR (PDB codes 2L6R and 2L6B) and rSR (PDB codes 2L6C and 3HMK) [101]. The cartoon representation of hSR tertiary structure is depicted in Figure 5. hSR consists of two main domains that form the active site [57]. The enzyme can occur in two different conformations – open conformation, when the active site is empty, and closed conformation, when the active site is occupied by either substrate or competitive inhibitor. In the case of hSR crystallized in order to collect X-ray data, malonate as one of the most potent inhibitors of SR (see Chapter 1.4.5) was bound into the active site and the conformation of the enzyme was thus closed (see Figure 5, p. 17). In accordance with the fact that SR is considered as PLP-dependent enzyme (see Chapter 1.4.1), the active site of hSR X-ray structure contains PLP covalently bound to the enzyme by a Schiff base linkage with K56 residue. Finally, the presented hSR structure includes Mn^{2+}. Although manganese is not believed to activate hSR *in vivo*, the structure reveals the plausible coordination of any divalent cation. This is carried out in an octahedral manner by three conserved residues (E210, D216 and A214) and three water molecules.

In solution, SR does not remain as a monomer but multimerizes into dimers and tetramers [85,90]. Interestingly, none of the reported SR activators influence the formation of SR quaternary structure suggesting that neither reducing agents nor divalent cations or ATP are necessary for stabilization of the SR multimerization state [85,88,90-91].

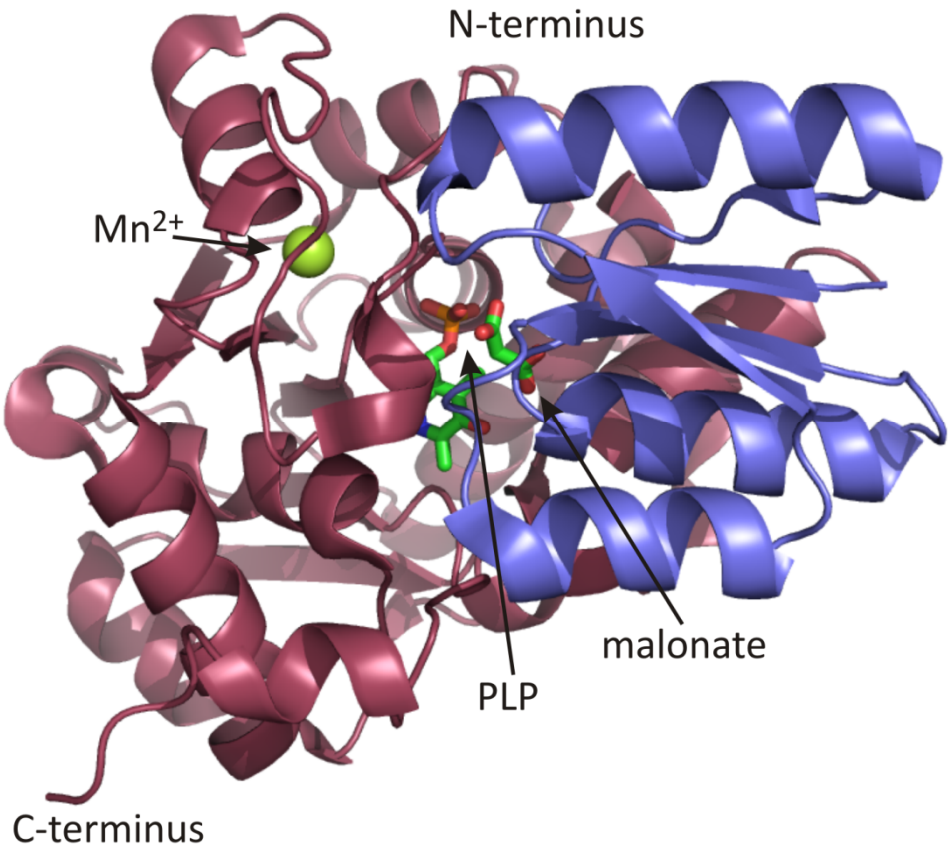

Figure 5: 3D structure of human serine racemase. Cartoon representation shows large domain (purple, residues 1-68 and 157-340) and small domain (blue, residues 78-115) which together form the active site of the enzyme. The active site is occupied by PLP and malonate. To the cation site, Mn^{2+} (shown as a green sphere) is bound. The image was prepared in PyMol program [102] using the structure under the 3L6B PDB code.

1.4.5. Inhibitors of serine racemase

Considering the possible involvement of SR in pathology of several neurological diseases (see Chapter 1.3.4), it is not surprising that this enzyme has become a promising target of pharmaceutical intervention. Indeed, it is assumed that specific inhibition of SR in neuropathological conditions would lead to reduction of D-serine in the brain resulting in decrease of NMDA receptor overactivation. However, to date, efforts aiming to find potent SR inhibitors have been fruitless since the most effective compounds exhibit a micromolar K_i (see Table 3, p. 18). Moreover, vast majority of the inhibitory studies have been conducted on mSR. The differences between the behaviour of mSR and hSR are though believed to be negligible since it has been shown that both enzymes display comparable inhibitor sensitivity [85].

Table 3: The most potent inhibitors of serine racemase identified so far.

INHIBITOR	STRUCTURE	SR tested	K_i (μM)	REF.
L-*erythro*-3-hydroxyaspartate	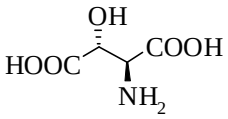	mSR hSR	43 ± 7 11 ± 1	[84] [85]
malonate	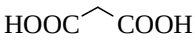	mSR hSR	71 ± 16 33 ± 3	[84] [85]
L-aspartic acid *β*-hydroxamate	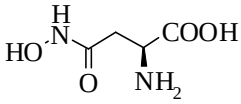	mSR	98 ± 24	[103]
positive hit n.9	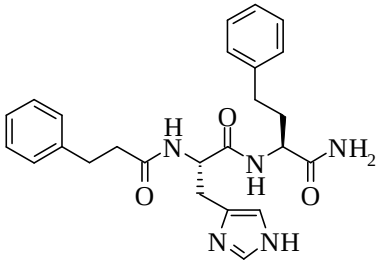	hSR	320 ± 70	[104]
maleate	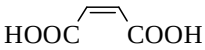	mSR	550 ± 120	[84]
positive hit n.11	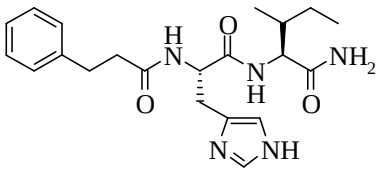	hSR	610 ± 120	[104]
L-cysteine-*S*-sulfate	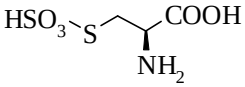	mSR	640 ± 140	[84]
meso-tartrate	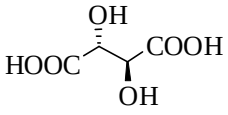	mSR	660 ± 100	[84]
dihydroxyfumarate	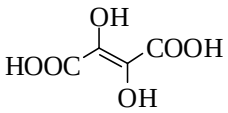	mSR	690 ± 50	[84]
L-asparagine	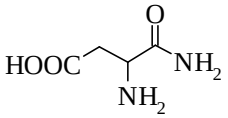	mSR	1130 ± 30	[84]

During the searching for a potent SR inhibitor, several different strategies have been employed. Most of the studies focused on systematic modification of L-serine and L-serine-*O*-sulfate [84,90]. However, screenings of wide panel of amino acids [75,105], small peptides [104] and other miscellaneous compounds structurally unrelated to serine [89,103] have been also performed.

The testing of L-serine and L-serine-*O*-sulfate based compounds has revealed the most potent inhibitors identified so far and also suggested the structural features necessary for efficient binding of a ligand to SR. It was observed that the L-serine derivatives formed by addition of electronegative groups to the *β*-carbon usually possess higher affinity towards SR than L-serine itself [84]. Moreover, the presence of electronegative substituent such as amino or hydroxyl group on the α-carbon can even strengthen the binding efficiency. However, in some cases, the removal of α-amino substituent from the serine scaffold does not lead to decrease of the affinity. Indeed, even though malonate does not carry any substituent on the α-carbon, it possesses one of the highest inhibitory efficiency towards SR published so far (see Table 3) [84].

The typical representative of SR inhibitor meeting both main rules mentioned above is L-*erythro*-3-hydroxyaspartate (see Table 3). As the most potent inhibitor of SR identified to date, this compound has been recently successfully employed in cell culture and *in vivo* experiments. L-*erythro*-3-hydroxyaspartate was shown to be capable of blocking the synthesis of D-serine in primary astrocyte cell culture [36]. Moreover, this compound was also utilized to demonstrate that its injection into the rats suffering from arthritic pain leads to reduction of the levels of D-serine in the brain, which results in alleviation of the signs of the neurotoxicity [106].

Following the rules for efficient binding of a ligand to SR, the stereoisomers of L-*erythro*-3-hydroxyaspartate should have a similar inhibitory efficiency. Indeed, L-*threo*-3-hydroxyaspartate has been shown to dramatically decrease SR activity. However, rather than a typical competitive inhibitor, this compound acts as the SR substrate during *β*-elimination (see Chapter 1.4.1.2) [84]. As for D-isomers of 3-hydroxyaspartates, D-*threo*-3-hydroxyaspartate displayed neither substrate nor inhibitory activity and the experimental data for D-*erythro*-3-hydroxyaspartate are not yet available [89].

L-aspartic acid *β*-hydroxamate, the derivate of 3-hydroxyaspartate, has been also determined as one of the most effective inhibitors of SR published to date (see Table 3) [103]. In fact, other hydroxamic acids have been shown to possess high inhibitory activity towards SR as well. However, many of them act non-specifically since they inhibit also other PLP-dependent enzymes [103].

It is obvious that none of the SR inhibitors identified so far can be used in clinical practice since the amount of the compound necessary for effective inhibition of SR is very high. However, some of the SR ligands such as malonate, L-*erythro*-3-hydroxyaspartate and L-aspartic acid *β*-hydroxamate could serve as lead compounds in further inhibitor development studies. In this context, a rational drug design performed with the 3D structure of hSR could be also very helpful.

2. AIMS AND OBJECTIVES

Since most of current inhibitors of serine racemase are weak and little is known about their specificity, it is desirable to search for novel ligands of this enzyme. Therefore, the main aim of this study was to test wide panel of different compounds for their inhibitory efficiency toward mouse serine racemase and identify a potential lead compound for further development.

The objectives are as follows:

1. To express, purify and characterize mouse serine racemase (mSR).
2. To analyze the ability of different compounds to inhibit mSR.
3. To investigate the most potent inhibitors further in terms of binding affinity and mechanism of action.
4. To identify potential substrates of mSR.
5. To determine kinetic constants for these novel substrates of mSR.

3. MATERIALS AND METHODS

3.1. Materials

3.1.1. Chemicals

acetic acid ..... Penta (Prague, CZ)
acetone .....Lachema (Brno, CZ)
acetonitrile ..... Penta (Prague, CZ)
acrylamide.....Sigma (St. Louis, USA)
adenosine-5'-triphosphate (ATP).....Sigma (St. Louis, USA)
ammonium persulfate .....Serva (Heidelberg, Germany)
ammonium sulfate.....Lachema (Brno, CZ)
ampicillin .....Sigma (St. Louis, USA)
boric acid..... USB (Cleveland, USA)
bromphenol blue .....Sigma (St. Louis, USA)
Coomassie Brilliant Blue G-250.....Serva (Heidelberg, Germany)
chloric acid..... Penta (Prague, CZ)
dinitrophenylhydrazine (DNPH)..... Fluka (Buchs, Switzerland)
dithiothreitol (DTT) .....Sigma (St. Louis, USA)
ethanol..... Penta (Prague, CZ)
ethylene glycol.....Lachema (Brno, CZ)
FDAA, Marfey's Reagent (1-fluoro-2-4-dinitrophenyl-5-L-alanine amide).....
.....Thermo Fisher Scientific (Waltham, USA)
formic acid .....Sigma (St. Louis, USA)
glycerol ..... Penta (Prague, CZ)
glycine.....Duchefa (Haarlem, Netherlands)
HEPES (4-(2-hydroxyethyl)-1-piperazineethanesulfonic acid).....
.....Sigma (St. Louis, USA)
hydrogen chloride ..... Penta (Prague, CZ)
α-ketoglutarate .....Sigma (St. Louis, USA)
magnesium chloride.....Lachema (Brno, CZ)
2-mercaptoethanol .....Sigma (St. Louis, USA)

methanol..... Penta (Prague, CZ)
N,N'-methylen-bis(acrylamide) ..... USB (Cleveland, USA)
o-phenylenediamine.....Sigma (St. Louis, USA)
potassium bicarbonate.....Lachema (Brno, CZ)
potassium chloride .....Sigma (St. Louis, USA)
potassium dihydrogen phosphate.....Lachema (Brno, CZ)
potassium hydroxide..... Penta (Prague, CZ)
pyridoxal-5´-phosphate (PLP) .....Sigma (St. Louis, USA)
L-serine, D-serine .....Sigma (St. Louis, USA)
sodium acetate trihydrate..... Penta (Prague, CZ)
sodium azide ..... Penta (Prague, CZ)
sodium deoxycholate .....Serva (Heidelberg, Germany)
sodium dodecyl sulfate .....Sigma (St. Louis, USA)
sodium chloride.....Lachema (Brno, CZ)
sodium hydroxide ..... Penta (Prague, CZ)
sodium hydrogen phosphate .....Lachema (Brno, CZ)
sulphuric acid..... Penta (Prague, CZ)
TBA (tetrabutylammonium) .....Sigma (St. Louis, USA)
TEA (triethanolamine).....Sigma (St. Louis, USA)
TEMED (tetramethylethylendiamine) ..... Fluka (Buchs, Switzerland)
Tris (tris(hydroxymethyl)aminomethane)..... USB (Cleveland, USA)
triton X-100.....Serva (Heidelberg, Germany)
Tween 20..... USB (Cleveland, USA)

3.1.2. Compounds for inhibition testing

The compounds for the inhibition studies on mSR were purchased from commercial sources (Sigma-Aldrich or Alfa Aesar), prepared by Petr Jansa and Jiří Schimer from Institute of Organic Chemistry and Biochemistry (IOCB) or obtained from a research group of prof. Carlo De Micheli (University of Milan). For the list of compounds containing the code, structure, name and the source of the compound see Table 4.

Table 4: List of compounds analyzed in the study.

CODE	STRUCTURE	NAME	SOURCE
M1	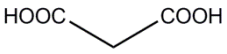	malonic acid	Sigma-Aldrich
M2	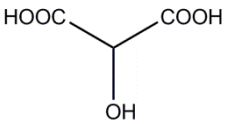	2-hydroxymalonic acid	Alfa Aesar
M3	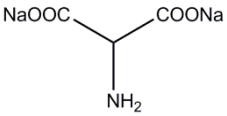	sodium 2-aminomalonate	Petr Jansa
M4	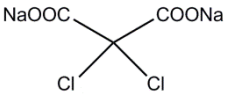	sodium 2,2-dichloromalonate	Petr Jansa
M5	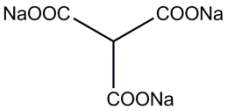	sodium 2-carboxymalonate	Petr Jansa
M6	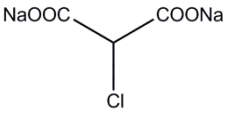	sodium 2-chloromalonate	Petr Jansa
M7	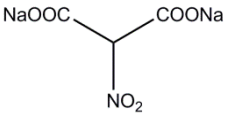	sodium 2-nitromalonate	Petr Jansa
M8	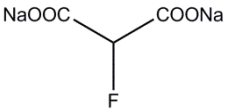	sodium 2-fluoromalonate	Petr Jansa
M9	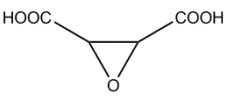	epoxysuccinic acid	Sigma-Aldrich

M10	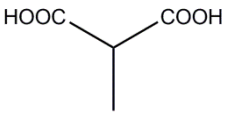	2-methylmalonic acid	Sigma-Aldrich
M11	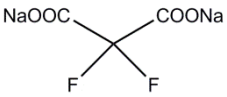	sodium 2,2-difluoromalonate	Jiří Schimer
M12	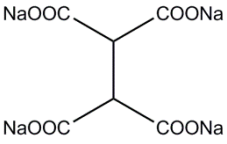	sodium ethane-1,1,2,2,-tetracarboxylate	Petr Jansa
M13	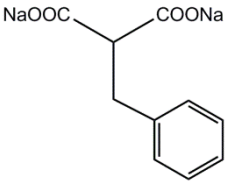	sodium 2-benzylmalonate	Petr Jansa
M14	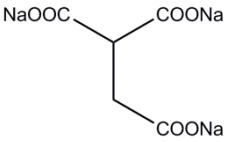	sodium 2-carboxymethyl malonate	Petr Jansa
M15	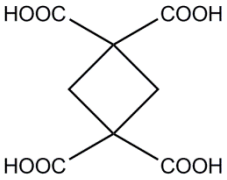	cyclobutane-1,1,3,3-tetracarboxylic acid	Sigma-Aldrich
M16		2,2-dimethylmalonic acid	Sigma-Aldrich
M17	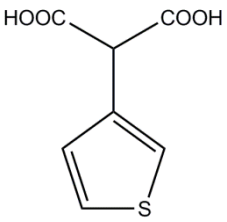	2-(3-thiophene)malonic acid	Sigma-Aldrich
M18	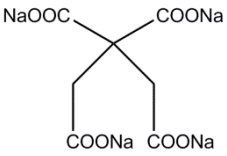	sodium 2,2-bis(carboxymethyl)malonate	Petr Jansa
M19	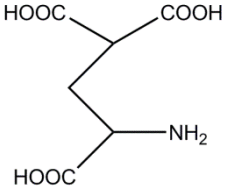	γ-carboxy-DL-glutamic acid	Sigma-Aldrich

M20	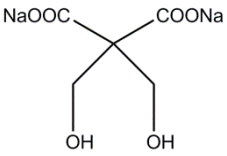	sodium 2,2-bis(hydroxymethyl)malonate	Petr Jansa
M21	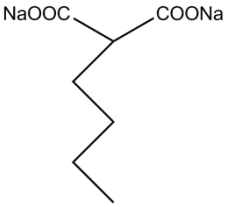	sodium 2-butylmalonate	Petr Jansa
G1	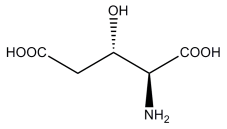	L-*erythro*-3-hydroxyglutamic acid	prof. Carlo De Micheli
G2	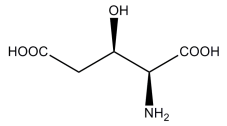	L-*threo*-3-hydroxyglutamic acid	prof. Carlo De Micheli
G3	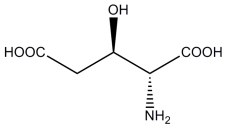	D-*erythro*-3-hydroxyglutamic acid	prof. Carlo De Micheli
G4	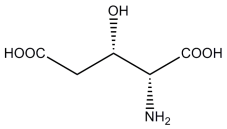	D-*threo*-3-hydroxyglutamic acid	prof. Carlo De Micheli
G5	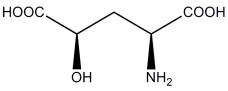	L-*threo*-4-hydroxyglutamic acid	prof. Carlo De Micheli
G6	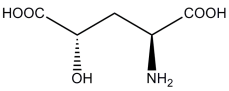	L-*erythro*-4-hydroxyglutamic acid	prof. Carlo De Micheli
G7	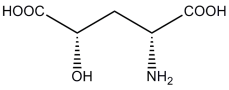	D-*threo*-4-hydroxyglutamic acid	prof. Carlo De Micheli
G8	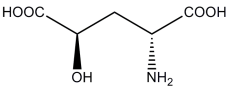	D-*erythro*-4-hydroxyglutamic acid	prof. Carlo De Micheli
G9	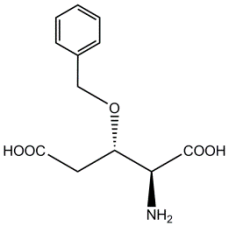	L-*erythro*-3-benzyloxy-glutamic acid	prof. Carlo De Micheli

G10	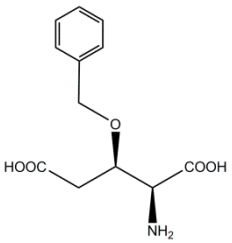	L-*threo*-3-benzyloxy-glutamic acid	prof. Carlo De Micheli
G11	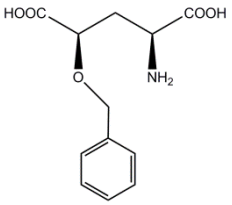	L-*threo*-4-benzyloxy-glutamic acid	prof. Carlo De Micheli
R1	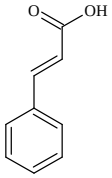	cinnamic acid	Petr Jansa
R2	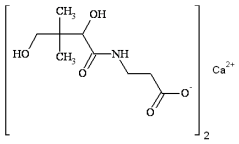	calcium pantothenate	Petr Jansa
R3	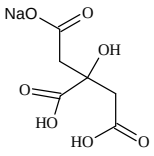	sodium citrate	Petr Jansa
R4	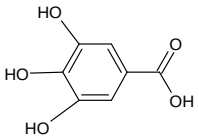	gallic acid	Petr Jansa
R5	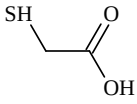	thioglycolic acid	Petr Jansa
R6	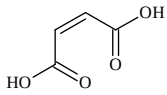	maleic acid	Petr Jansa
R7	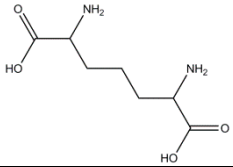	diaminopimelic acid	Petr Jansa
R8	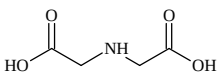	iminodiacetic acid	Petr Jansa

R9	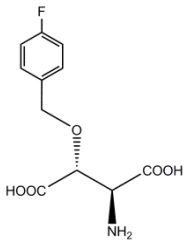	L-*erythro*-3-(4-fluorobenzyl) oxy-aspartic acid	prof. Carlo De Micheli
R10	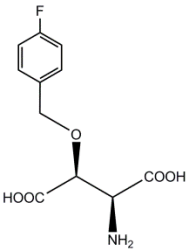	L-*threo*-3-(4-fluorobenzyl) oxy-aspartic acid	prof. Carlo De Micheli
R11	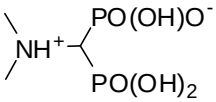	hydrogen((dimethylammonio) (phosphono)methyl) phosphonate	Petr Jansa
R12	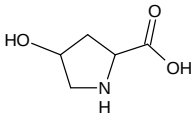	4-hydroxyproline	Petr Jansa
R13	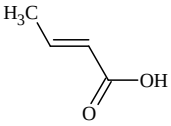	crotonic acid	Petr Jansa
R14	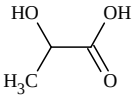	2-hydroxypropionic acid	Petr Jansa
R15	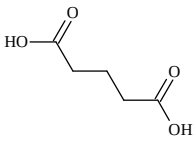	glutaric acid	Petr Jansa
R16	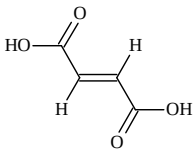	fumaric acid	Petr Jansa
R17	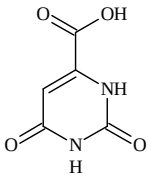	orotic acid	Petr Jansa
R18	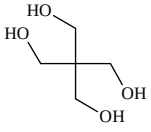	pentaerythritol	Petr Jansa

3.1.3. Instruments

autoclave:	MLS-3020U (Tokyo, Japan)
CCD camera:	LAS-3000 CCD Camera, Fujifilm (Tokyo, Japan)
centrifuges:	Biofuge Pico, Heraeus Instruments (Hanau, Germany)
	Centifuge 5415R, Eppendorf (Hamburg, Germany)
	Beckman J2-MI, Beckman Coulter (Brea, USA)
	Sorvall Evolution RC, Thermo Scientific (Waltham, USA)
chromatography:	ÄKTA explorer, Amersham Pharmacia Biotech (Uppsala, Sweden)
HPLC:	
– instruments:	Alliance HPLC High Throughput, Waters (Milford, USA)
	Rapid Resolution LC Series 1200, Agilent (Santa Clara, USA)
– detectors:	Dual Wavelength Absorbance Detector, Waters (Milford,USA)
	1200 Series Fluorescence Detector, Agilent (Santa Clara, USA)
Laboratory scales:	AE 163, Mettler (Greifensee, Switzerland)
	EK-400H, A&D Engineering, Inc. (San Jose, USA)
pH-meter:	9450 pH meter, Unicam (Cambridge, UK)
rotary incubator:	Innova 4300, New Brunswick Scientific (Enfield, USA)
sonicator:	Soniprep 150, Sanyo (Tokyo, Japan)
spektrophotometers:	GENios, Tecan (Männedorf, Switzerland)
	UV-VIS Spectrophotometer SPECORD 21O, Analytik Jena (Jena, Germany)
thermostats:	Grant Instruments Ltd**.** (Shepreth, UK)
	Thermomix BU, B.Braun (Melsungen, Germany)
Vertical Polyacrylamid Gel Eletrophoresis:	Sigma (St. Louis, USA)
Western blot apparatus:	Trans-Blot SD, Bio-Rad (Hercules, USA)

3.1.4. Other material

ATP-agarose ..... Sigma (St. Louis, USA)
L-arabinose ..... Sigma (St. Louis, USA)
Blocker Casein ..... Thermo Fisher Scientific (Waltham, USA)
BSA (bovine serum albumin) ..... Imuna (Šarišské Michaľany, SK)
Centriprep YM-30..... Amicon, Millipore Corporation (Billerica, USA)
Complete Mini, EDTA free, Protease inhibitor cocktail tablets.....
..... Roche (Basel, Switzerland)
Chemoluminiscence substrate WestFemto ..... Thermo Fisher Scientific (Waltham, USA)
Dialysis membrane Spectra/Por, MWCO 6-8 kDa ..... Serva (Heidelberg, Germany)
DNaseI ..... Roche (Basel, Switzerland)
Glucose Nutrient Mix ..... AthenaES (Baltimore, USA)
HPLC columns:

- Eclipse Plus C_{18} ..... Agilent Technologies (Santa Clara, USA)
- Symmetry C_{18} (4,6×250 mm), particles 5 µm..... Waters (Milford,USA)

Hyper Broth ..... AthenaES (Baltimore, USA)
LB agar ..... Sigma (St. Louis, USA)
LB medium ..... Sigma (St. Louis, USA)
lysozyme ..... Serva (Heidelberg, Germany)
Phenyl-Sepharose FastFlow..... Pharmacia (Stockholm, Sweden)
Q-Sepharose..... Pharmacia (Stockholm, Sweden)
transparent 96-well microplate with flat bottom..... Koh-i-noor (České Budějovice, CZ)
SDS marker..... Serva (Heidelberg, GERMANY)

Antibodies

- primary antibody 3B7.1
  - monoclonal anti-human serine racemase antibody
  - prepared by EXBIO (Prague, CZ) using inclusion bodies with recombinant human serine racemase with his-tag produced in *E.coli*
  - supernatant, total amount of proteins 140 mg/ml
  - for basic characterization of this antibody see [107]

– secondary antibody

- goat anti-mouse antibody conjugated with horseradish peroxidase (0.8 mg/ml)..... .....Thermo Fisher Scientific (Waltham, USA)

Bacterial strain: *E.coli* MC1061, ATCC (Manassas, USA)

Plasmid pA4_mSR (for more information about the plasmid see [84])

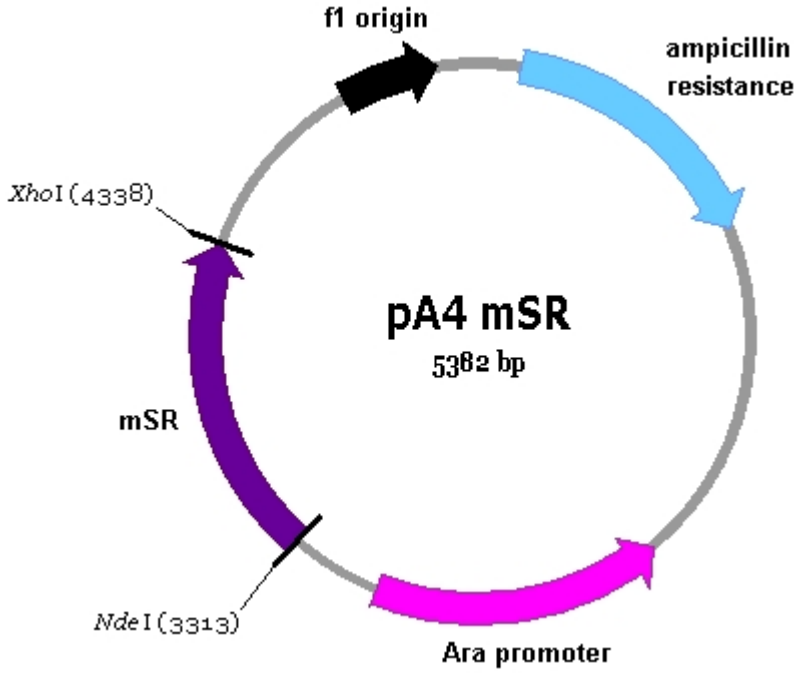

3.2. Methods

3.2.1. Mouse serine racemase expression

Mouse serine racemase was expressed using competent *E.coli* MC1061 and pA4_mSR plasmid encoding mouse serine racemase. The pA4_mSR transformation into *E.coli* MC1061 and subsequent mSR expression were performed according to [84]. 2 µl of pA4_mSR plasmid solution (DNA concentration 1024 ng/µl) was added into 100 µl of competent cells. Mixture was incubated for 5 minutes on ice and then 90 seconds at 42°C followed by 1 minute incubation on ice. 1 ml of sterile Luria-Bertani Broth (LB) medium was added into the tube with cells and solution was incubated for 45 minutes at 37°C. Finally, the mixture was spread onto 12 LB Agar plates supplemented by ampicillin (final concentration 100 µg/ml) and bacteria were left to grow over night at 37°C.

Growth medium for mSR production was prepared using 15.6 g of Hyper Broth and 350 ml of deionized water per one 2 l Erlenmayer flask (12 flasks were prepared in total). After sterilisation, growth medium was supplemented by Glucose Nutrient Mix (final concentration 10 mg/ml) and ampicillin (final concentration 100 µg/ml). 800 µl of growth medium was then added into each plate with bacteria grown over night and colonies were harvested using hockey-stick. Cell suspension was collected in the sterile 15 ml tube and subsequently split equally into all flasks containing growth medium.

The bacteria were grown at 37°C and 300 rpm and OD_{595} of the cell suspension was measured each hour. When OD_{595} reached a value of 0.9, mSR production was induced by 1mM L-arabinose. Five hours after induction, cell cultures were harvested by centrifugation (12000×*g*, 10 min, 4°C), supernatant was discarded and pellet was stored at -80°C.

3.2.2. mSR purification

3.2.2.1. Cell lysis

The cell pellet obtained from mSR expression was thawed on ice and 200 ml of QA buffer (20mM triethanolamine hydrochloride-NaOH, pH 7.0, 20 μM pyridoxal-5‘-phosphate, 1 mM $MgCl_2$, 100 μM DL-dithiothreitol and 0.02% (w/v) NaN_3) supplemented by the Complete Mini, EDTA-free, Protease inhibitor mix were added. To suspend the cell pellet Dounce homogenizer was used. The cell suspension was incubated with 200 μg/ml chicken egg lysozyme for 1 hour at room temperature before appropriate amount of 2% (w/v) sodium deoxycholate was added to gain a final concentration of 0.05%. Suspension was then gently shaken for additional 20 minutes followed by addition of DNaseI to a final concentration of 10 μg/ml. The sample was sonicated on ice 3 times for 30 s with 30s intervals between cycles and centrifuged at 18480×g and 4°C for 20 minutes. Soluble fraction (supernatant) was then used for further purification of mSR using ammonium sulfate precipitation, reversed-phase chromatography, ion-exchange chromatography and affinity chromatography.

3.2.2.2. Ammonium sulfate precipitation

The pH of saturated solution (approximately 4.1 M) of ammonium sulfate was adjusted to 7.2 using saturated solution of NaOH. 160 ml of the prepared ammonium sulfate solution was then slowly dripped (a drop at a time) into 240 ml of soluble fraction of cell lysate followed by centrifugation of the mixture at 18480×g and 4°C for 20 minutes. Since analysis of the pellet and supernatant using SDS polyacrylamide electrophoresis (see Chapter 3.2.3.2) revealed that the mSR precipitated from the solution (see Chapter 4.1.1.) the non-soluble fraction was used for further mSR purification. The pellet was suspended in 300 ml of QA buffer and centrifuged at 18480×g and 4°C for 20 minutes.

3.2.2.3. Reversed-phase chromatography

A Phenyl-Sepharose FastFlow column was pre-equilibrated with 3 column volumes of QA buffer. The supernatant containing mSR was applied onto the column in a flow rate of 8-10 ml/min. The column was then washed by 3 column volumes of QA buffer before bound proteins were eluted with 50% (v/v) ethylene glycol in QA buffer (pH 7.0). The fractions

containing mSR were combined and immediately diluted with an equal volume of QA buffer.

3.2.2.4. Ion-exchange chromatography

A Q-Sepharose FastFlow column was pre-equilibrated with one column volume of distilled water, two column volumes of QB buffer (QA buffer supplemented by 0.5 M KCl, pH 7.0) and finally two column volumes of QA buffer. Diluted fractions from reversed-phase chromatography were loaded onto the column in a flow rate of 3-4 ml/min. The column was subsequently washed by five column volumes of QA buffer before bound proteins were eluted in a linear gradient of 0 – 100 % QB buffer in QA buffer. The fractions containing mSR were combined and dialysed in dialysis tubes (Spectra/Por) of molecular weight cut-off 6-8 kDa overnight against 400 volumes of QA buffer at 4°C.

3.2.2.5. Affinity chromatography

An ATP-agarose column was pre-equilibrated with three column volumes of QA buffer. The dialysed mSR solution was loaded onto the column in a flow rate of 5 ml/min. The column was washed by three column volumes of QA buffer and bound mSR was eluted by 2 column volumes of 2 mM ATP in QA buffer (pH 7.0). The fractions containing mSR were combined and dialysed in dialysis tubes of molecular weight cut-off 6-8 kDa overnight against 500 volumes of QA buffer at 4°C. mSR solution was then concentrated 200-fold and stored in 50 µl aliquots at -80°C.

3.2.3. Assessment of mSR purity and enzymatic activity

3.2.3.1. Determination of protein concentration

The protein concentration in a sample was determined using Bradford protein assay [108]. All measurements were conducted in a 96-well transparent microplate and each serial dilution was performed in duplicates.

For a calibration, an inner standard bovine serum albumin (BSA) was used. 160 µl of 50 µg/ml BSA solution was added into the well containing 160 µl of water. The BSA solution in a concentration of 25 µg/ml was then diluted in 2-fold serial dilutions leading to a standard curve of 25, 12.5, 6.25, 3.13, 1.57 and 0.78 µg/ml.

For the determination of a total protein concentration in the sample, 40 µl of the sample was added into the well containing 160 µl of water. The solution was then diluted in 5-fold serial dilutions to gain 5 different sample dilutions.

Finally, 40 µl of 5× Coomassie Brilliant Blue G-250 was added into each well and solutions were mixed thoroughly with a multichannel pipette. After 5 minutes incubation at room temperature, the absorbance was measured at 595 nm on the GENios microplate reader (Tecan) and concentrations of each sample were calculated using Magellan programme (Tecan).

3.2.3.2. Sodium dodecyl sulfate-polyacrylamide gel electrophoresis (SDS-PAGE)

Discontinuous SDS-PAGE was used for analysis of the samples taken from mSR expression and each step of purification. All gels consisted of 12% resolving gel and 5% stacking gel.

The mixture for 12% resolving gel contained 375 mM Tris-HCl (pH 8.8), 12% (v/v) acrylamide mixture (acrylamide with N,N'-bisacrylamide in the ratio 35.7:1), 0.1% (w/v) SDS, 0.1% (w/v) ammonium persulfate (APS) and 0.01% (v/v) TEMED.

The mixture for 5% stacking gel contained 250 mM Tris-HCl (pH 6.8), 5% (v/v) acrylamide mixture (acrylamide with N,N'-bisacrylamide in a ratio 35.7:1), 0.1% (w/v) SDS, 0.1% (w/v) ammonium persulfate (APS) and 0.02% (v/v) TEMED.

After polymerisation, gels were placed into an electrophoresis apparatus (Sigma) and both the upper and the lower reservoir were filled by SDS Running Buffer (25 mM Tris, pH 8.8, 250 mM glycine, 0.1% SDS). Prior to the loading into the gel, the samples were mixed with loading buffer (350 mM Tris, pH 6.8, 30% glycerol, 10% SDS, 0.6% 2-mercaptoethanol, 1.2% bromphenol blue) in the ratio 5:1 and boiled for 5 minutes. Electrophoresis was run at a constant voltage of 150 V until the bromphenol blue dye reached the bottom of the gel. The separated proteins were visualized either by Commassie Briliant Blue staining or using Western blot.

3.2.3.3. Commassie Briliant Blue staining of polyacrylamide gel

Polyacrylamide gel containing separated proteins was incubated in Commassie Briliant Blue solution (0.1% Coomassie Brilliant Blue R-250, 50% methanol, 10% acetic acid) for 30 minutes at room temperature with a gentle agitation and subsequently destained using 10% acetic acid. The destaining solution was replenished several times until background of the gel was fully destained. Stained gels were scanned on the scanner (Canon).

3.2.3.4. Western blotting using semi-dry transfer

Once the SDS-PAGE (Chapter 3.2.3.2) was finished, the gel was equilibrated together with nitrocellulose membrane and 4 sheets of filter paper in a transfer buffer (25 mM Tris-HCl, 192 mM glycine, 10% methanol, 0.1% SDS) for 10 minutes at room temperature. The blotting sandwich was subsequently made by placing two sheets of filter paper onto the anode of the transfer apparatus followed by nitrocellulose membrane, gel and additional two sheets of filter paper. To eliminate the bubbles between the layers, a test tube was rolled over the upper filter paper. The cathode was then placed on top of the blotting sandwich and transfer apparatus was closed. Proteins were transferred at constant voltage of 15 V for 15 min.

After electroblotting, the membrane was blocked in 4 ml of Blocker Casein for 1 hour at room temperature with a gentle agitation and subsequently incubated in primary antibody 3B7.1 (for more information about the antibody see Chapter 3.1.4) diluted in a ratio 1:20 in Blocker Casein overnight at 4˚C with the gentle agitation. The membrane was then washed with PBS and 0.05% Tween three times and incubated with secondary antibody (for more information about the antibody see Chapter 3.1.4.) diluted 1:20,000 in Blocker Casein for 1 hour at room temperature. After another washing, the blot was incubated with 700 µl of SuperSignal West Femto Maximum Sensitivity Substrate (ThermoScientific) for 5 minutes, dried between two sheets of filter paper and developed using chemiluminiscence CCD camera LAS-3000 (Fujifilm).

3.2.3.5. Determination of specific activity of mSR

Serine racemase specific activity in samples from different steps of purification was assessed using a natural substrate of the enzyme L-serine. Enzymatic reactions were carried out at 37°C in a pH 8.0 buffer containing 100 mM HEPES-NaOH,

10 μM pyridoxal-5'-phosphate, 1 mM $MgCl_2$, 5 mM DL-dithiothreitol, 1 mM ATP and 5 mM L-serine. The reactions were started by addition of the sample from the particular purification step. The amount of total protein (as determined by Bradford assay, see Chapter 3.2.3.1) added to the reaction depended on the stage of purification. The total volume of the reaction was 100 µl. The reactions were stopped by addition of 20 µl 1.8 M $HClO_4$ after 25 min and neutralized by 20 µl of 1.8 M KOH. Glycine was added as an internal standard and mixtures were cooled down at -20°C.

The formation of a product (D-serine) as well as the amount of substrate (L-serine) left and the presence of internal standard (glycine) were analyzed by reversed-phase HPLC (Alliance HPLC, Waters and Dual Wavelength Absorbance Detector, Waters) after pre-column derivatization.

Reaction mixtures were first thawed at room temperature and centrifuged for 5 minutes at 16100×g. 10 µl of the sample was then mixed with 5 µl of 1 M $KHCO_3$ and 25 µl of 1-fluoro-2-4-dinitrophenyl-5-L-alanine amide (FDAA) and reactions were incubated at 45°C for at least 45 minutes. Derivatization was stopped by addition of 2 M HCl to a final concentration of 250 mM and the solutions were subsequently diluted 10 times by 50% methanol. Mixtures were centrifuged for 10 minutes at 16100×g and 300 µl of each sample was pipetted into the auto sampler. Symmetry C18 Column (4.6×250mm, particle size 5 µm, Waters) used for the measurements was first equilibrated in a flow rate 1 ml/min with a mobile phase containing 32.5 mM sodium acetate, pH 4.4 and 35% methanol for 30 minutes. 50 µl of the sample was then analyzed in 35 – 98% of methanol gradient in 65 – 2 % of 50 mM sodium acetate, pH 4.4. The flow rate was 1ml/min and the running time was 20 min. The amino acid derivatives were detected by ultraviolet (UV) absorption at 340 nm.

The amount of D-serine formed in each reaction was determined using a calibration curve of D-serine and the specific activities *s.a.* were subsequently calculated from the equation:

$$s.a. = \frac{n_{D-serine}[\mu\text{mol}]}{m_{total\ protein}[\text{mg}] \cdot t[\text{min}]},$$

where $n_{D-serine}$ is the amount of D-serine formed, $m_{total\ protein}$ is the amount of total protein in the sample and t is reaction time.

3.2.3.6. Measurements of kinetics of L-serine racemisation

The enzymatic reactions were performed at 37°C in a pH 8.0 buffer containing 100 mM HEPES-NaOH, 10 µM pyridoxal-5'-phosphate, 1 mM $MgCl_2$, 5 mM DL-dithiothreitol, 1 mM ATP and 10 µg/ml (~135 nM) mSR and either 1 mM or 15 mM L-serine). The total volume of the reaction was 100 µl. All measurements were performed in duplicates. The reactions were started by addition of the substrate and stopped by addition of 20 µl 1.8 M $HClO_4$ after 5.7, 11.4, 16.3, 20.8, 26.7, 30.7, 45.7 and 63.5 minutes. The solutions were subsequently neutralized by 20 µl of 1.8 M KOH and cooled down at -20°C.

The samples were derivatized and the amino acid (D-serine and L-serine) derivatives were resolved on Symmetry C18 reversed-phase HPLC Column as described in Chapter 3.2.3.5. The amount of a product D-serine produced in the reactions was normalized to the amount of total serine (L-serine + D-serine) and the values obtained were used for investigation of the dependence of the amount of product made over time.

3.2.3.7. Determination of kinetic constants for L-serine racemisation

The enzymatic reactions were performed at 37°C in a pH 8.0 buffer containing 100 mM HEPES-NaOH, 10 µM pyridoxal-5'-phosphate, 1 mM $MgCl_2$, 5 mM DL-dithiothreitol, 1 mM ATP and 10 µg/ml (~135 nM) mSR. The concentration of L-serine varied from 15 µM to 2 mM. The total volume of the reaction was 100 µl. All measurements were performed in duplicates. The reactions were started by addition of the substrate and stopped by addition of 20 µl 1.8 M $HClO_4$ after 25 min. The solutions were subsequently neutralized by 20 µl of 1.8 M KOH and cooled down at -20°C.

The samples were derivatized and the amino acid (D-serine and L-serine) derivatives were resolved on Symmetry C18 reversed-phase HPLC Column as described in Chapter 3.2.3.5. The amount of D-serine formed in each reaction was determined using a calibration curve of D-serine and the initial velocities v_0 were subsequently calculated from the equation:

$$v_0 = \frac{c_{D-serine}[\mathrm{mM}]}{t[\mathrm{min}]},$$

where $c_{D-serine}$ is the amount of D-serine formed and t is the reaction time. To obtain K_m

and V_{max} values, the dependence of initial velocities on initial substrate concentration was fitted into the Michaelis-Menten equation by nonlinear regression using GraFit program, version 5 (Erithacus Software Limited) [109]. k_{cat} value was subsequently determined using equation:

$$k_{cat} = \frac{V_{\max}[\mu\mathrm{M} \cdot \mathrm{min}^{-1}]}{E_0[\mu\mathrm{M}]},$$

where V_{max} is the maximum reaction rate of mSR as determined by GraFit and E_0 is the concentration of mSR in the reaction.

3.2.4. Testing of compounds for their inhibitory efficiency towards mSR

3.2.4.1. Preparation of the compound solutions

Compounds (for the list of compound see Chapter 3.1.2) were dissolved in water to gain 100 mM final concentrations. In some cases, addition of DMSO or 10 M NaOH was necessary for a complete dissolution of the compound. The solutions were stored at -20°C.

3.2.4.2. Inhibition analysis

Enzymatic activities of mSR in the presence of tested compound were determined as described in [84]. Briefly, activity reactions were carried out at 37°C in a pH 8.0 buffer containing 100 mM HEPES-NaOH, 10 μM pyridoxal-5'-phosphate, 1 mM $MgCl_2$, 5 mM DL-dithiothreitol, and 1 mM ATP. The concentration of mouse serine racemase was always 10 µg/ml (~135 nM), while the concentrations of L-serine and tested compounds depended on the type of experiment. In the initial screening, the concentrations of both L-serine and tested compound were equal – 5 mM.

To determine IC_{50} values, 10 different inhibitor concentrations were used, while the concentration of L-serine remained constant at 5 mM. The suitable concentrations for each inhibitor were chosen based on the results of previous screening.

In the experiments for determination of mechanism of inhibition and K_i, different concentrations of L-serine (ranging from 1 mM to 15 mM) as well as inhibitor (ranging from 0 mM to 150 mM) were used.

The volume of reaction mixtures was 100 µl. All measurements were performed in duplicates. Reactions were started by addition of substrate, stopped by addition of 20 µl 1.8 M $HClO_4$ after 10 – 25 min and neutralized by 20 µl of 1.8 M KOH. Glycine was added as the internal standard and samples were cooled down at -20°C.

The samples were derivatized and the amino acid (D-serine, L-serine and glycine) derivatives were resolved on Symmetry C18 reversed-phase HPLC Column as described in Chapter 3.2.3.5.

3.2.4.3. Result processing

Once the reaction mixtures from the initial screening were resolved using HPLC, the amount of the product D-serine formed in the reactions was normalized either to the amount of the internal standard glycine or to the amount of total serine (D-serine + L-serine) and the values obtained were used for calculation of $v_{i,0}/v_0$ as follows:

$$\frac{v_{i,0}}{v_0} = \frac{n_{norm.\ D-serine,inh.}}{n_{norm.\ D-serine}},$$

where $n_{norm.\ D-serine,inh.}$ is the normalized amount of D-serine formed in the presence of the tested compound and $n_{norm.\ D-serine}$ is the normalized amount of D-serine formed in the absence of tested compounds.

In the case of IC_{50} and K_i value measurements, $v_{i,0}/v_0$ value was first determined and the obtained data were then used for calculation of inhibition constants by GraFit 5.0.4 (Erithacus Software Limited) [109].

3.2.5. Enzymatic measurements with novel mSR substrates

3.2.5.1. Testing of compounds as possible substrates of mSR

The enzymatic reactions were performed at 37°C in a pH 8.0 buffer containing 100 mM HEPES-NaOH, 10 µM pyridoxal-5'-phosphate, 1 mM $MgCl_2$, 5 mM DL-dithiothreitol, 1 mM ATP, 10 µg/ml (~135 nM) mSR and 5 mM compound tested.

The volume of reaction mixtures was 100 µl. All measurements were performed in duplicates. Reactions were started by addition of substrate, stopped by addition of 20 µl 1.8 M $HClO_4$ after 30 minutes and neutralized by 20 µl of 1.8 M KOH. The samples were cooled down at -20°C.

Formation of the expected product α-ketoglutarate was determined by reversed-phase HPLC (Alliance HPLC, Waters and Dual Wavelength Absorbance Detector, Waters) after pre-column derivatization.

Reaction mixtures were thawed at room temperature and centrifuged for 5 minutes at 16100×g. 25 µl of the sample was then mixed with 25 µl of dinitrophenylhydrazine (DNPH, Fluka) solution (13.5 µM DNPH, 1.3% H_2SO_4, 6.5% ethanol, 45% methanol) and 450 µl of 50% (v/v) methanol was subsequently added into the mixture. The solutions were incubated at room temperature for 5 minutes and then centrifuged for 10 minutes at 16100×g and 4°C. 400 µl of each sample was pipetted into the auto sampler. Symmetry C18 Column (4.6×250mm, particle size 5 µm, Waters) used for the measurements was first equilibrated in a flow rate 1 ml/min with a mobile phase containing 30 mM tetrabutylammonium hydroxide adjusted to pH 4.3 by ultrapure acetic acid and 40% methanol for 30 minutes. 50 µl of the sample was then analyzed in 40 – 85% of methanol gradient in 60 – 15 % of 50 mM tetrabutylammonium hydroxide, pH 4.3. The flow rate was 1ml/min and the running time was 32 min. The α-ketoglutarate derivatives were detected by ultraviolet (UV) absorption at 366 nm.

3.2.5.2. Determination of kinetic constants for novel substrates of mSR

Activity reactions were performed in duplicates at 37°C in a pH 8.0 buffer containing 100 mM HEPES-NaOH, 10 μM pyridoxal-5'-phosphate, 1 mM $MgCl_2$, 5 mM DL-dithiothreitol, and 1 mM ATP. The concentration of mouse serine racemase and

hydroxyglutamate depended on the compound tested (mSR ranging from 10 nM to 790 nM, substrate ranging from 25 µM to 20 mM). Reactions were started by addition of substrate and stopped by addition of 20 µl 1.8 M $HClO_4$ after a defined time (5 – 15 minutes depending on compound used).

Formation of the product α-ketoglutarate was determined by reversed-phase HPLC (Rapid Resolution LC Series 1200, Agilent and 1200 Series Fluorescence Detector, Agilent) after pre-column derivatization.

Reaction mixtures were mixed with derivatization reagent (10 mg/ml *o*-phenylenediamine, Sigma in 0.5 M HCl) in a 1:1 ratio, incubated at 110°C for 10 minutes and cooled down. Eclipse Plus C_{18} Column (2.1×50mm, particle size 1.8 µm, Agilent Technologies) used for the measurements was first equilibrated in a flow rate 0.4 ml/min with a mobile phase containing 0.1% formic acid and 23% acetonitrile for 10 minutes. The mixtures were then analyzed in 23 – 100% of acetonitrile gradient with 0.1% formic acid in 77 – 0% of 0.1% formic acid. The flow rate was 0.4 ml/min and the running time was 5 min. The α-ketoglutarate derivative was detected by fluorescence detector, where excitation wavelength was set up on 340 nm leading to emission in 420 nm.

The amount of α-ketoglutarate formed in each reaction was calculated using a calibration curve of α-ketoglutarate and the initial velocities v_0, K_m, V_{max} and k_{cat} values were determined as described in Chapter 3.2.3.7.

4. RESULTS

4.1. Preparation and kinetic characterization of recombinant mSR

4.1.1. mSR preparation

Recombinant mouse serine racemase was prepared using *E.coli* expression system and 4-step purification – precipitation by ammonium sulfate, reversed-phase chromatography on Phenyl-Sepharose, ion-exchange chromatography on Q-Sepharose and affinity chromatography on ATP-agarose.

The result of each purification step is shown in Figure 6. The cells were first lysed in a lysis buffer (for more details see Chapter 3.2.2.1). However, the mSR solubilisation was not achieved completely since significant amount of the enzyme remained in a non-soluble fraction (see Figure 6). Despite this fact, only a soluble fraction was used for further purification.

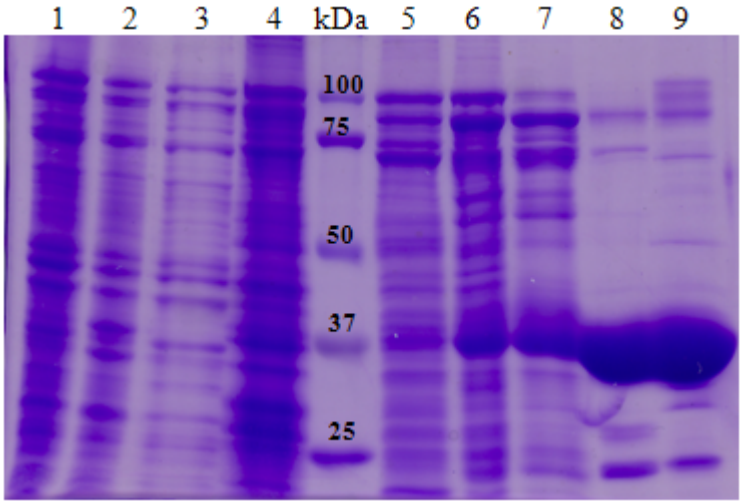

Figure 6: Summary of the mouse serine racemase purification. The SDS-PAGE gel with individual fractions from each purification step stained by Commasie blue. The samples were boiled in the loading buffer and resolved using 12% SDS-PAGE as described in the Chapter 3.2.3.2. Total amount of a protein in a well was 10 µg. The molecular weight of mSR is around 37 kDa. Lanes: 1 – cell lyzate non-soluble fraction, 2 – cell lyzate soluble fraction, 3 – soluble fraction from ammonium sulfate precipitation, 4 – non-soluble fraction from ammonium sulfate precipitation, 5 – supernatant obtained after dissolution of non-soluble fraction from ammonium sulfate precipitation in the lysis buffer, 6 – eluate from reversed-phase chromatography on Phenyl-Sepharose, 7 – eluate from ion-exchange chromatography on Q-Sepharose, 8 – eluate from affinity chromatography on ATP-agarose, 9 – mSR standard.

In contrast with a 3-step purification procedure published by our research group [84], the precipitation step using saturated solution of ammonium sulfate was included before proceeding to the purification by chromatographic techniques. Previous observations showed that mSR precipitates from a solution when the concentration of ammonium sulfate reaches 50% (v/v) (data not shown). Since it was desirable to keep mSR in the solution, the appropriate amount of saturated ammonium sulfate leading to 40% final concentration (v/v) was added into the cell lysate. However, the analysis of the samples using SDS polyacrylamide electrophoresis revealed that mSR precipitated from the solution completely (see Figure 6, p. 43). The non-soluble fraction obtained after precipitation step was thus suspended in an appropriate amount of lysis buffer again and the supernatant was used for further purification. The combination of reversed-phase chromatography, ion-exchange chromatography and affinity chromatography resulted in mSR solution in a purity of around 80% (see Figure 6, p. 43). The increasing efficiency of the purification was also monitored by determination of mSR specific activity in the samples after each purification step (Figure 7A).

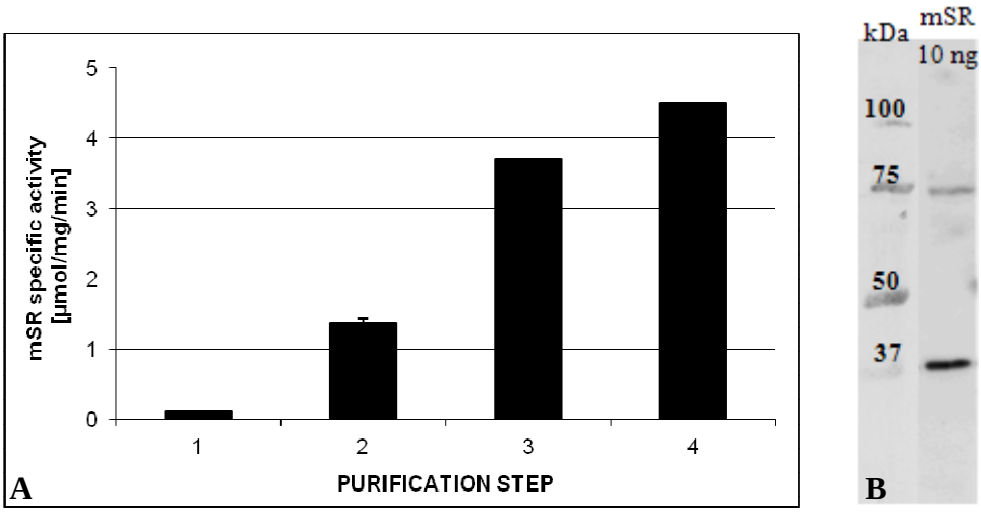

Figure 7: Monitoring of mouse serine racemase purification. The presence of the mSR in a sample after each purification step was confirmed by determination of mSR specific activity using L-serine as a substrate (**panel A**). The appropriate amount of the sample was incubated in a pH 8.0 buffer containing 100 mM HEPES-NaOH, 10 μM pyridoxal-5'-phosphate, 1 mM $MgCl_2$, 5 mM DL-dithiothreitol, 1 mM ATP and 5 mM L-serine. The amount of D-serine formed was determined by reversed-phase HPLC. 1 – supernatant obtained after dissolution of non-soluble fraction from ammonium sulfate precipitation in a lysis buffer, 2 – eluate from reversed-phase chromatography, 3 – eluate from ion-exchange chromatography, 4 – eluate from affinity chromatography. The presence of mSR in a final solution was also confirmed by Western blotting (**panel B**). The mSR was detected using antibody 3B7.1.

The appropriate amount of the sample was incubated in a reaction buffer (see Chapter 3.2.3.5) with 5 mM substrate (L-serine) for 25 minutes at 37°C. The amount of the D-serine formed was then used for the calculation of mSR specific activity in each sample. It was determined that the specific activity of mSR increased during the purification 40 times. To confirm the presence of mSR in the final solution with an independent analytical method, Western blot was performed leading to the detection of two bands – the band corresponding with the molecular weight of mouse serine racemase (around 37 kDa) and the band of the molecular weight of 75 kDa approximately (Figure 7B, p. 44).

4.1.2. Kinetic characterization of the recombinant mSR

To ensure that the purified mSR possesses kinetic properties comparable to those published previously, the enzyme kinetics of L-serine racemisation was investigated. The enzyme assay utilized in all experiments throughout kinetic characterization of mSR and inhibition studies was based on end-point measurement of the product. For this reason, it was desirable to first determine the reaction time in which the amount of product increases linearly over time and the reaction velocity can be thus considered as initial.

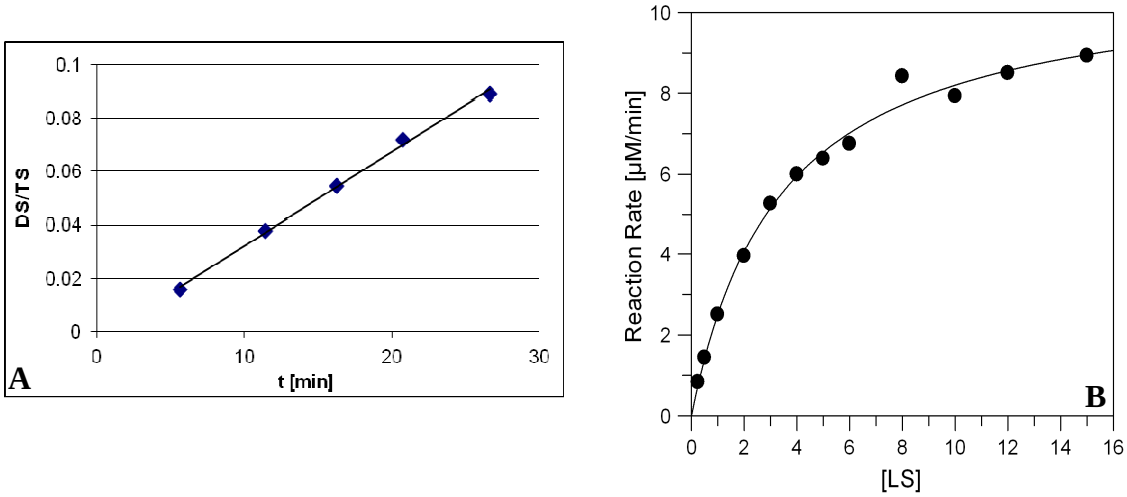

Figure 8: Kinetic characterization of recombinant mSR during racemisation reaction. Panel A: The dependence of the amount of D-serine made during the racemisation reaction over time. DS/TS values represent the amounts of D-serine normalized to total serine (L-serine + D-serine). **Panel B:** The dependence of initial velocities on initial substrate concentrations during the racemisation of L-serine (LS) to D-serine catalyzed by mSR. The data were fitted using program GraFit 5.0.4 (Erithacus Software Limited) [109].

The mouse serine racemase in a concentration of 135 nM was incubated in the reaction buffer (see Chapter 3.2.3.6) with 2 different L-serine concentrations (1 mM and 15 mM) for 8 different times (ranging from 5 minutes to 65 minutes) at 37°C and the amount of the product D-serine produced in each time point was then investigated.

It was determined that the reaction time for L-serine in the concentration of 1 mM should be kept under 30 minutes in order to ensure that kinetic measurement is conducted within the initial reaction velocity (Figure 8A, p. 45). A similar trend was also observed when the concentration of L-serine was 15 mM (data not shown).

The Michaelis-Menten kinetics of mSR during racemisation of L-serine to D-serine was subsequently measured using 12 different concentrations (ranging from 0.25 mM to 15 mM) of substrate. The amount of the product (D-serine) formed during the reaction was then used for calculation of initial reaction rate and the data obtained were processed by GraFit 5.0.4 (Erithacus Software Limited) [109]. An example of the graphical representation showing dependence of the initial reaction rates of L-serine racemisation on the initial L-serine concentration is depicted in Figure 8B (p. 45).

Apart from generating of Michaelis-Menten kinetics hyperbolic plot, GraFit 5.0.4 also calculates K_m and V_{max} values. K_m value for L-serine racemisation was determined as 3.4 ± 0.3 mM. The V_{max} value (11.0 ± 0.4 μM/min) was then used for calculation of k_{cat} (68.9 ± 2.2 min^{-1}) and k_{cat}/K_m (20 ± 2 $min^{-1}mM^{-1}$) values.

4.2. Inhibition studies on mSR

In order to search for a potent inhibitor of racemisation reaction catalyzed by mSR, 50 compounds were tested. The chemicals were either purchased from commercial sources or prepared by Petr Jansa and Jiří Schimer from IOCB or obtained from a research group of prof. Carlo De Micheli (University of Milan). These compounds can be divided into 3 groups – malonate-based compounds, hydroxyglutamates and their derivatives and miscellaneous compounds selected from chemical library of Petr Jansa.

All compounds were first tested in a 5 mM ligand prescreening where mSR in a concentration of 135 nM was incubated in a reaction buffer (see Chapter 3.2.4.2) with equimolar amount of compound and L-serine substrate (5 mM) for less than 25 minutes at

37°C. The amount of D-serine product produced in the reaction was then used for calculation of $v_{i,0}/v_0$ ($v_{i,0}$ is the relative enzymatic activity in the presence and v_0 in the absence of the compound). The compounds which decreased the racemisation activity of serine racemase by more than 98% were further characterized using IC_{50} and K_i value measurements. The details of a reaction setup for these measurements will be mentioned where appropriate.

4.2.1. Malonate-based compounds

From 21 compounds (compounds M1-M21, for the structures see Chapter 3.1.2) tested in 5 mM ligand prescreening, 7 compounds (M1 – M7) showed high inhibition potency towards mSR ($v_{i,0}/v_0 < 0.2$), 10 compounds (M8 – M17) appeared to be moderate inhibitors ($v_{i,0}/v_0 = 0.2 – 0.7$) and 4 compounds (M18 – M21) had almost no inhibitory effect on racemisation reaction ($v_{i,0}/v_0 > 0.7$) (see Figure 9).

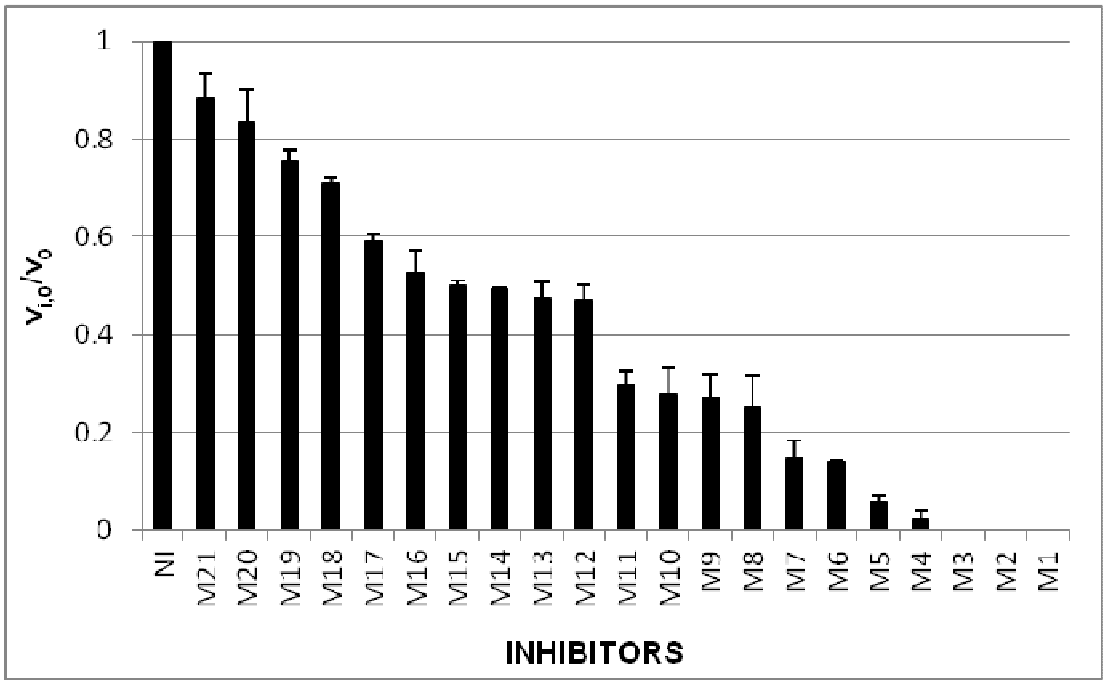

Figure 9: Inhibition of mSR racemisation reaction by malonate-based compounds. Activity reactions were carried out at 37°C in a pH 8.0 buffer containing 100 mM HEPES-NaOH, 10 μM pyridoxal-5'-phosphate, 1 mM $MgCl_2$, 5 mM DL-dithiothreitol, 1 mM ATP, 135 nM mSR, 5 mM L-serine and 5 mM compound tested. NI – non inhibited reaction. For the structures of compounds see Chapter 3.1.2. $v_{i,0}/v_0$ value represents the ability of tested compound to decrease the activity of mSR ($v_{i,0}$ is the relative enzymatic activity in the presence and v_0 in the absence of the compound).

To determine IC_{50} values of the four most potent inhibitors (M1 – M4), the activity of serine racemase was analyzed in the presence of 10 different compound concentrations ranging from 0.001 mM to 7.5 mM. The concentration of L-serine was kept constant at 5 mM. The $v_{i,0}/v_0$ values for each reaction were then utilized for calculation of IC_{50} values using GraFit 5.0.4 (Erithacus Software Limited) [109]. The graphical representation for the most effective inhibitor 2,2-dichloromalonate (M4), showing dependence of the $v_{i,0}/v_0$ value on the inhibitor concentration, is depicted in Figure 10A (p. 48). IC_{50} values of all four inhibitors tested are summarized in Table 5.

Table 5: IC_{50} values of the most potent malonate-based inhibitors of mSR. Activity testing was carried out at 37°C in a pH 8.0 buffer containing 100 mM HEPES-NaOH, 10 μM pyridoxal-5'-phosphate, 1 mM $MgCl_2$, 5 mM DL-dithiothreitol, 1 mM ATP, 135 nM mSR and 5 mM L-serine. The inhibitory potency of each compound was measured in 10 different concentrations, the concentration range was chosen based on the previous 5 mM prescreening.

CODE	STRUCTURE	NAME	IC_{50} [μM]
M1	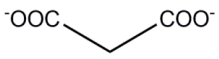	malonate	67 ± 1
M4	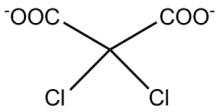	2,2-dichloromalonate	57 ± 1
M2	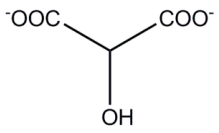	tartronate	94 ± 1
M3	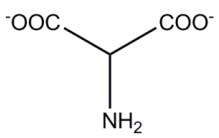	2-ammonium malonate	400 ± 100

Considering the results of IC_{50} value measurements, malonate and 2,2-dichloromalonate were selected for further investigation of the mechanism of inhibition using double reciprocal Lineweaver-Burk plot [110]. For this purpose, the activity of mSR was analyzed in the presence of 6 different concentrations of L-serine (ranging from 1 mM to 15 mM)

and 3 different concentrations of inhibitor (ranging from 0 mM to 150 mM). The data were processed by GraFit 5.0.4 (Erithacus Software Limited) [109] which also enables the K_i value calculation.

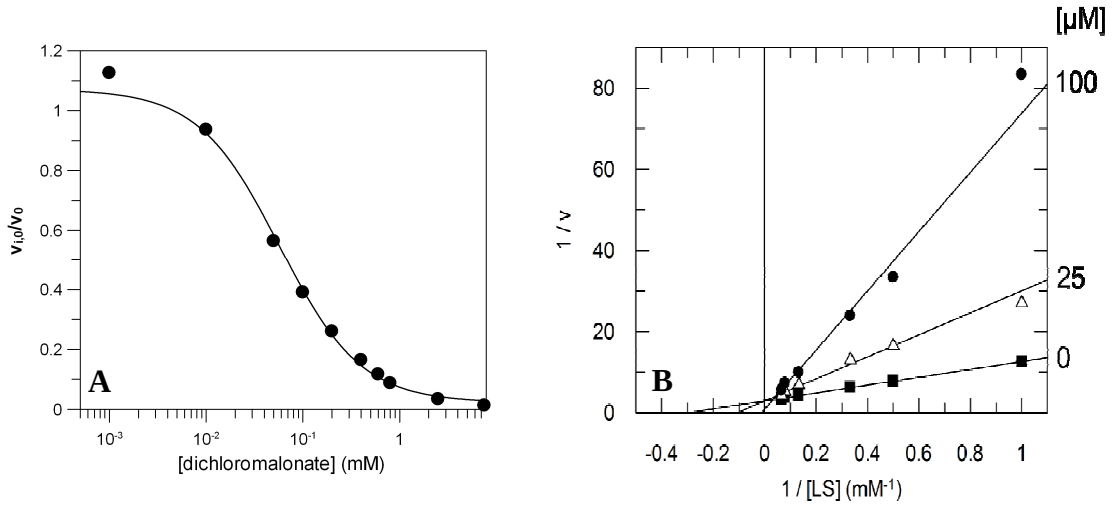

Figure 10: Characterization of the most potent inhibitor of mSR 2-dichloromalonate. Panel A: The non-linear fit for determination of IC_{50} value of 2-dichloromalonate. **Panel B:** Double reciprocal Lineweaver-Burk plot showing the competitive mechanism of inhibition of mSR by 2-dichloromalonate. LS = L-serine. Data were processed by program GraFit 5.0.4 (Erithacus Software Limited) [109].

The example of the Lineweaver-Burk plot for the most potent inhibitor 2,2-dichloromalonate is shown in Figure 10B. Both compounds appeared to be competitive inhibitors with K_i value being 19 ± 3 µM for 2,2-dichloromalonate and 27 ± 3 µM for malonate.

Apart from the further exploration of inhibitors that decreased the racemisation activity of mSR in the 5 mM ligand prescreening by more than 98%, the IC_{50} values of some weaker inhibitors were also determined and are summarized in Table 6 (p. 50). The range of concentrations for each inhibitor differed and was chosen based on the results of 5 mM ligand prescreening.

Table 6: IC_{50} values of some weaker malonate-based inhibitors of mSR. Activity testing was carried out at 37°C in a pH 8.0 buffer containing 100 mM HEPES-NaOH, 10 μM pyridoxal-5'-phosphate, 1 mM $MgCl_2$, 5 mM DL-dithiothreitol, 1 mM ATP, 135 nM mSR and 5 mM L-serine. The inhibitory potency of each compound was measured in 10 different concentrations, the concentration range was chosen based on the previous 5 mM prescreening.

CODE	STRUCTURE	NAME	IC_{50} [μM]
M6	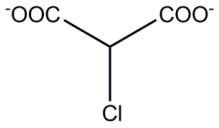	2-chloromalonic acid	780 ± 100
M7	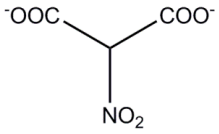	2-nitromalonic acid	1650 ± 490
M10	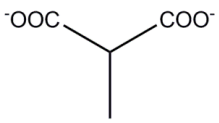	methylmalonic acid	1850 ± 210
M11	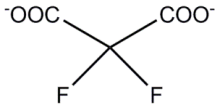	2,2-difluoromalonic acid	2160 ± 200
M16	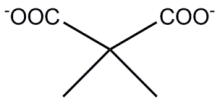	dimethylmalonic acid	5630 ± 510
M17	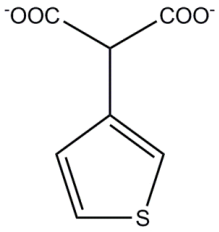	2-thiofenmalonic acid	7030 ± 480
M20	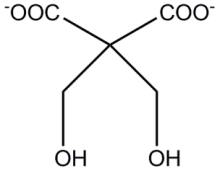	2,2-bis(hydroxymethyl)-malonic acid	40600 ± 11000

4.2.2. Hydroxyglutamates and their derivatives

Most of the hydroxyglutamate stereoisomers and their derivatives (compounds G1-G11, for the structures see Chapter 3.1.2) tested in 5 mM ligand prescreening inhibited the racemisation reaction catalyzed by mSR moderately or had no effect (see Figure 11). Only D-*threo*-3-hydroxyglutamate (compound G4) decreased the racemisation activity of mSR significantly.

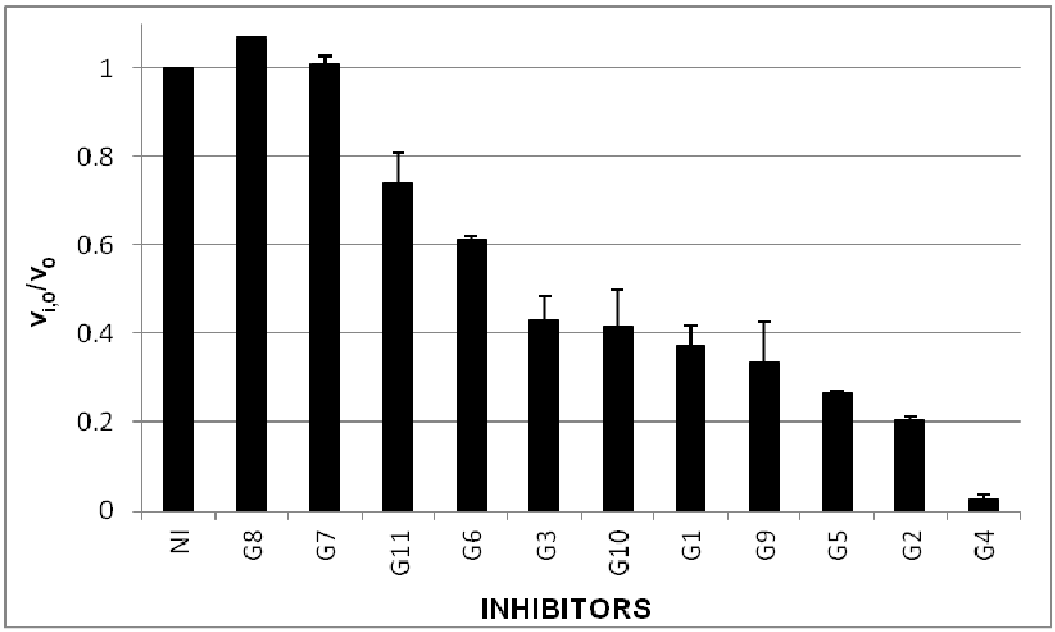

Figure 11: Inhibition of mSR racemisation reaction by hydroxyglutamates and their derivatives. Activity reactions were carried out at 37°C in a pH 8.0 buffer containing 100 mM HEPES-NaOH, 10 μM pyridoxal-5'-phosphate, 1 mM $MgCl_2$, 5 mM DL-dithiothreitol, 1mM ATP, 135 nM mSR, 5 mM L-serine and 5 mM compound tested. For the structures of compounds see Chapter 3.1.2. $v_{i,0}/v_0$ value represents the ability of tested compound to decrease the activity of mSR ($v_{i,0}$ is the relative enzymatic activity in the presence and v_0 in the absence of the compound).

Since the FDAA method used for determination of the amount of D-serine in the reaction mixture enables to detect all amino acids it was possible to investigate whether the concentrations of hydroxyglutamate-based compounds alter during the reaction. While no changes were observed in the concentration of 4-hydroxyglutamates (compounds G5 – G8) and hydroxyglutamate derivatives (G9 – G11), concentrations of all 3-hydroxyglutamates (compounds G1 – G4) were decreased. Moreover, the degradation of compounds G1 and G2 was much more efficient than the degradation of the physiological substrate of mSR L-serine (see Figure 12, p. 52). At the same time, no additional signals in chromatograms

suggesting racemisation of these compounds on α-carbon were observed. It was thus assumed that 3-hydroxyglutamates are substrates of mSR and might undergo *β*-elimination reaction. For further investigation of 3-hydroxyglutamates as novel substrate of mSR see Chapter 4.3.

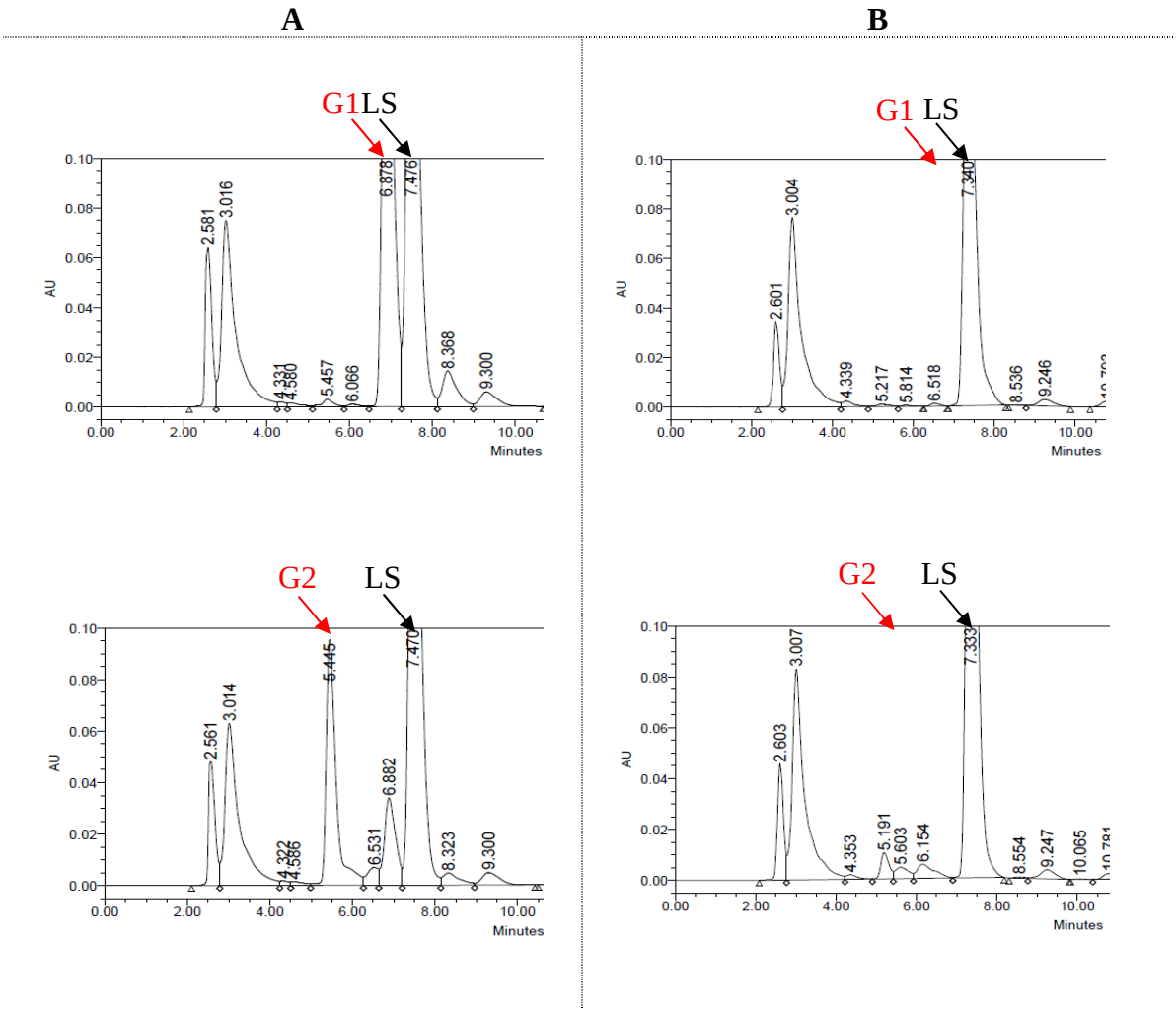

Figure 12: Degradation of 3-hydroxyglutamates in the presence of mSR. Tested compounds (G1 and G2, for structures of the compounds see Chapter 3.1.2) in the concentration of 5 mM were treated at 37°C in a pH 8.0 buffer containing 100 mM HEPES-NaOH, 10 μM pyridoxal-5'-phosphate, 1 mM $MgCl_2$, 5 mM DL-dithiothreitol, 1 mM ATP and 5 mM L-serine (LS) in the absence (column A) or presence (column B) of 135 nM mSR. The figure shows HPLC analyses of the reaction mixtures after pre-column derivatization by FDAA.

4.2.3. Miscellaneous compounds

From 18 compounds (compounds R1-R18, for the structures see Chapter 3.1.2) tested in the 5 mM ligand prescreening, 12 compounds (R1 – R12) appeared to be moderate inhibitors of mSR during racemisation reaction and 6 compounds (R13 – R18) had almost no effect (see Figure 13). Therefore, none of the compounds was further characterized using IC_{50} value and K_i value analysis. Interestingly, compounds R17 and R18 seemed to activate mSR. However, because of the high standard deviation the data were not convincing and the activation effect was thus not analyzed further.

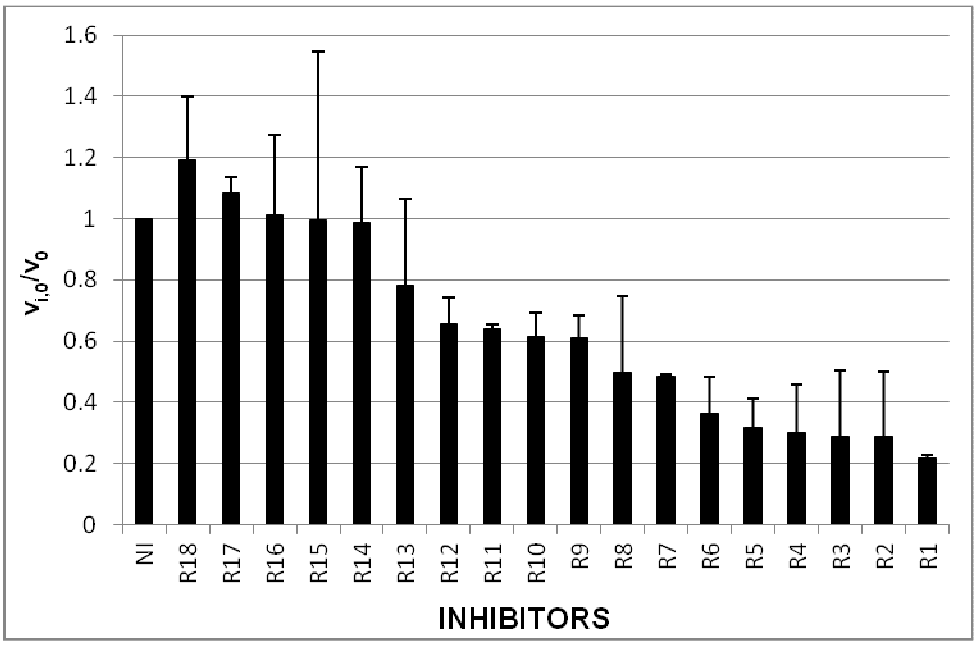

Figure 13: Inhibition of mSR racemisation reaction by hydroxyglutamates and their derivatives. Activity reactions were carried out at 37°C in a pH 8.0 buffer containing 100 mM HEPES-NaOH, 10 μM pyridoxal-5'-phosphate, 1 mM $MgCl_2$, 5 mM DL-dithiothreitol, 1 mM ATP, 135 nM mSR, 5 mM L-serine and 5 mM compound tested. NI – non inhibited reaction. For the structures of compounds see Chapter 3.1.2. $v_{i,0}/v_0$ value represents the ability of tested compound to decrease the activity of mSR ($v_{i,0}$ is the relative enzymatic activity in the presence and v_0 in the absence of the compound).

4.3. Novel substrates of mSR

To confirm the hypothesis that all four stereoisomers of 3-hydroxyglutamate are substrates of mSR β-elimination activity, mouse serine racemase in a concentration of 135 nM was incubated in a reaction buffer (see Chapter 3.2.5.1) with 5 mM compound at 37°C for 30 minutes. Reaction mixtures and solutions of 1 mM, 2.5 mM and 5 mM α-ketoglutarate (expected product of the reaction) were then derivatized by 2,4-dinitrophenylhydrazine (DNPH) and analyzed using reversed-phase HPLC. For the example of the chromatograms obtained from investigation of compound G1 as a potential substrate see Figure 14. The retention time for dinitrophenylhydrazine derivative of α-ketoglutarate was around 13.4 minutes (Figure 14A).

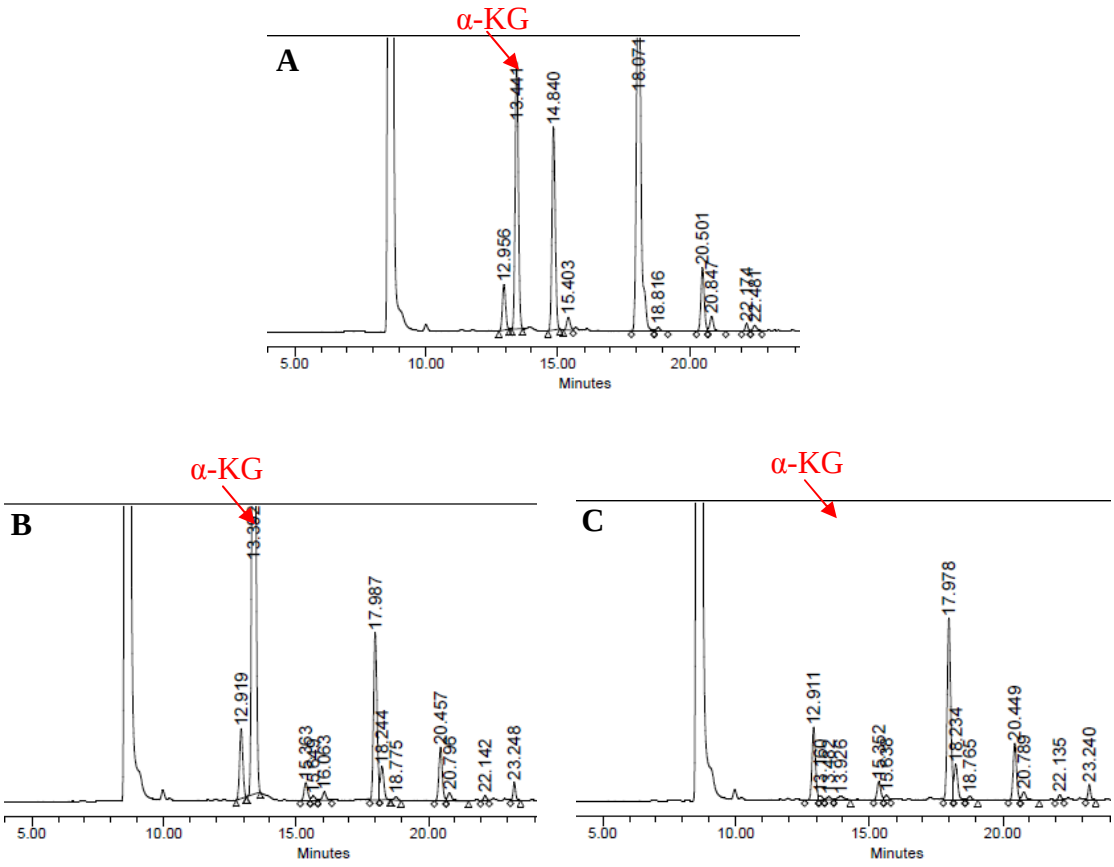

Figure 14: Generation of α-ketoglutarate (α-KG) from L-*erythro*-3-hydroxyglutamate during elimination reaction catalysed by mSR. Panel A: The chromatogram of 1 mM α-ketoglutarate after pre-column derivatization by 2,4-dinitrophenylhydrazine (DNPH). **Panel B:** HPLC analysis of L-*erythro*-3-hydroxyglutamate treated at 37°C in a reaction buffer (pH 8.0 buffer containing 100 mM HEPES-NaOH, 10 μM pyridoxal-5'-phosphate, 1 mM $MgCl_2$, 5 mM DL-dithiothreitol, 1 mM ATP) with 135 nM mSR. The solution was derivatized by DNPH before loading onto HPLC column. **Panel C:** HPLC analysis of L-*erythro*-3-hydroxyglutamate treated at 37°C in a reaction buffer without mSR. The solution was derivatized by DNPH before loading onto HPLC column.

No peak indicating the presence of α-ketoglutarate in the mixture when mSR was not added into the elimination reaction was visible in the chromatogram (Figure 14C, p. 54). On the other hand, after addition of the mSR into the reaction, a considerable amount of α-ketoglutarate was formed (Figure 14B, p. 54). Similar results were also generated using compounds G2 – G4 as the substrates (data not shown) suggesting that mSR indeed catalyzes the reaction of all 3-hydroxyglutamates to α-ketoglutarate.

It was thus desirable to determine a K_m value of each substrate. However, since the amount of α-ketoglutarate produced by 3-hydroxyglutamate elimination significantly differed according to substrate used, several optimisation reactions were first performed to ensure that all K_m measurements would be done within an initial reaction velocity. The most suitable mSR concentration, concentration range of 3-hydroxyglutamate and reaction time for each substrate are summarized in Table 7.

Table 7: Summary of the reaction conditions optimised for each mSR substrate.

CODE	NAME	concentration of mSR [nM]	reaction time [min]	concentration range of substrate [mM]
G1	L-*erythro*-3-hydroxyglutamate	10	5	0.025 - 5
G2	L-*threo*-3-hydroxyglutamate	16	10	0.125 - 20
G3	D-*erythro*-3-hydroxyglutamate	790	15	1 - 20
G4	D-*threo*-3-hydroxyglutamate	160	10	0.1 - 20

The data obtained from subsequent Michaelis-Menten kinetics measurements were very variable (data not shown). It was assumed that the inconsistent results could be caused by 2,4-dinitrophenylhydrazine derivatization. A new fluorescence-based HPLC method for detection of α-ketoglutarate in the reaction mixtures was thus developed by Radko Souček from IOCB. This detection method uses a pre-column derivatization of the samples by *o*-phenylenediamine (see Chapter 3.2.5.2). The Michaelis-Menten kinetics of mSR with

novel substrates was then measured using at least 6 different concentrations of the substrate (for concentration range see Table 7). The optimisation reactions for determination of the most suitable reaction conditions for each substrate were not repeated with the new HPLC detection method since it was supposed that they would not differ dramatically. To ensure that all measurements were conducted within the initial velocity, the percentage of substrate conversion was kept under 15%.

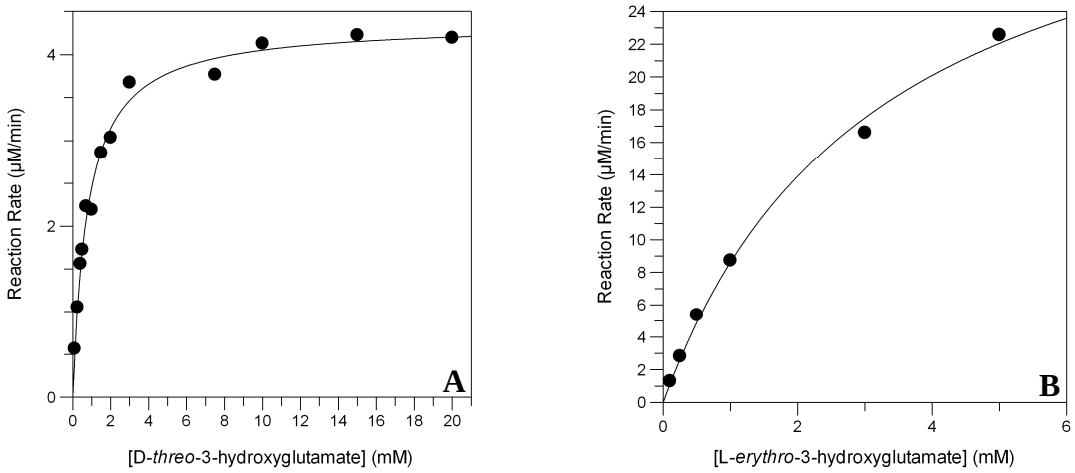

Figure 15: The dependence of initial velocities on initial substrate concentrations during the elimination of D-*threo*-3-hydroxyglutamate (A) and L-*erythro*-3-hydroxyglutamate (B) to α-ketoglutarate. The data were fitted using program GraFit 5.0.4 (Erithacus Software Limited) [109].

The amount of the α-ketoglutarate product formed during the reaction was then used for calculation of initial reaction rate and the data obtained were processed by GraFit 5.0.4 (Erithacus Software Limited) [109]. The graphical representations for compounds G1 and G4 showing dependence of the initial reaction rates of substrate elimination on the initial substrate concentration are depicted in Figure 15. K_m, k_{cat} and k_{cat}/K_m values for each substrate are summarized in Table 8 (p. 57).

Table 8: The Michaelis-Menten kinetics data of mSR with newly identified substrates.
Activity reactions were carried out at 37°C in a pH 8.0 buffer containing 100 mM HEPES-NaOH, 10 μM pyridoxal-5'-phosphate, 1 mM $MgCl_2$, 5 mM DL-dithiothreitol and 1 mM ATP. The concentration of mSR and the concentration range of the substrate in reaction is shown in Table 7 (p. 55).

SUBSTRATE	STRUCTURE	K_m [mM]	k_{cat} [min^{-1}]	k_{cat}/K_m [$min^{-1}mM^{-1}$]
L-*erythro*-3-hydroxyglutamate	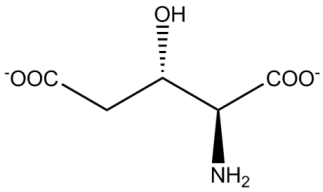	3.2 ± 0.5	3405 ± 254	1064 ± 184
L-*threo*-3-hydroxyglutamate	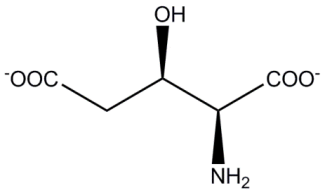	1.6 ± 0.1	317 ± 6	198 ± 13
D-*erythro*-3-hydroxyglutamate	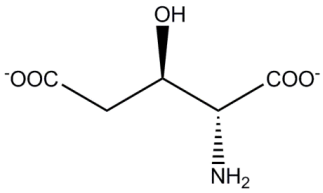	9.7 ± 1.5	123 ± 9	13 ± 2
D-*threo*-3-hydroxyglutamate	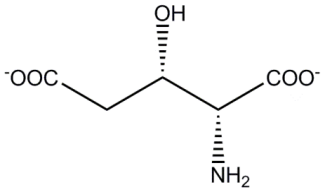	0.8 ± 0.1	26 ± 1	32 ± 4

5. DISCUSSION

Serine racemase as the enzyme responsible for the biosynthesis of a neurotrasmitter D-serine has become a promising target of pharmaceutical intervention in neurological diseases caused by overstimulation of NMDA receptors. However, no highly potent inhibitor of this enzyme has been identified to date and further search is thus desirable.

In this study, recombinant mouse SR was employed to screen 50 different compounds for their inhibitory potency. The utilization of human SR would be probably more appropriate since the preparation of its recombinant form has been already described [85]. However, in order to facilitate the comparison of the results with those already published, mSR, and not hSR, was exploited. Indeed, most of the inhibitory studies published so far have been conducted on the mouse ortholog of serine racemase. Nevertheless, mSR and hSR possess similar inhibitor specificity [85] and it can be thus assumed that any compound identified as a potent inhibitor of mSR would also effectively inhibit hSR.

Recombinant mSR was expressed by *E.coli* expression system and subsequently purified using ammonium sulfate precipitation and three different chromatography techniques. Since the enzyme construct does not contain any tag to enable one-step purification using affinity chromatography the preparation of mSR was rather time consuming. However, the modification of the enzyme by the tag could lead to alteration of its kinetic parameters and inhibitor specificity. The design of most of the compounds tested in this study was based on the mSR inhibitors published previously by our research group [84]. We thus decided to use the same construct for mSR expression.

The purification of mSR was then performed almost identically. The only exception represented the inclusion of the ammonium sulfate precipitation before proceeding to the purification by chromatography techniques. This led to preparation of the enzyme of higher purity than when only chromatography techniques were utilized (see Figure 6, p. 43, lane 8 vs. lane 9). However, the precipitation step extended the time of mSR purification even more and probably caused the loss of significant amount of expressed protein. Indeed, it was observed that the enzyme precipitated from the solution with lower concentration of ammonium sulfate than expected and most of the mSR thus appeared in non-soluble fraction. The subsequent solubilisation of the enzyme from this fraction was not achieved completely. The reason why the concentration of ammonium sulfate necessary for mSR

precipitation differed from the result determined previously is unclear. For further mSR preparation, the investigation of this phenomenon would be desirable.

The efficiency of the purification was monitored by SDS electrophoresis (see Figure 6, p. 43) and determination of specific activity of the enzyme in purification fractions (see Figure 7A, p. 44). With each purification step, the purity as well as specific activity of mSR increased indicating that the purification setup was chosen correctly. The presence of the enzyme in the final solution was independently confirmed by Western blotting (see Figure 7B, p. 44). However, along with the band corresponding with the molecular weight of mSR (37 kDa), the band of 2-fold molecular weight of mSR (75 kDa) was also detected. Since mSR is known to occur in solution in dimers [90], the presence of 75 kDa band on the developed blot could be caused by incomplete reduction of the sample prior loading into the SDS-PAGE gel. Nevertheless, it is assumed that mSR dimers are not stabilized by disulfide bridges [111] and the mentioned explanation of the presence of the 75 kDa band is thus improbable. It is more plausible that the detection of the protein with the molecular weight of 75 kDa is a result of antibody cross-reactivity since it has been shown that the primary antibody used for the identification of mSR is not completely specific [107].

The subsequent kinetic characterization of purified mSR revealed that the enzyme possesses the kinetic properties comparable to those published previously [84]. Indeed, K_m, k_{cat} and k_{cat}/K_m values for the L-serine to D-serine racemisation reaction of newly prepared mSR and mSR from the publication are 3.4 vs. 3.8 mM, 68.9 vs. 45.5 min^{-1} and 20 vs. 12 $min^{-1}mM^{-1}$.

Once the recombinant mSR was prepared and characterized, we searched for an effective inhibitor of this enzyme. The design of the compounds used in the study was based on previously published inhibitors or intuition that particular small molecules could fit into the active site of mSR. The structures of selected compounds can be thus grouped into three subsets – malonate-based compounds (Table 4, p. 24, compounds M1-M21), hydroxyglutamates and its derivatives (Table 4, p. 24, compounds G1-G11), and miscellaneous compounds (Table 4, p. 24, compounds R1-R18).

None of the compounds from the third mentioned group showed significant inhibitory potency towards mSR (Figure 13, p. 53). Within this group, fluorbenzyloxy derivatives of L-3-hydroxyaspartates were also tested. Since L-*erythro*-3-hydroxyaspartate is known to

be the most potent mSR inhibitor and L-*threo*-3-hydroxyaspartate was shown to be a substrate of mSR [84] both ligands could serve as lead compounds for further inhibitor development. However, the modification of hydroxyl group with the bulky moiety is not probably a strategy which would result in increase of the affinity towards mSR. Indeed, neither L-*erythro*-3-(4-fluorobenzyl)oxy-aspartate (compound code R9) nor L- *threo*-3-(4-fluorobenzyl)oxy-aspartate (compound code R10) were capable of efficient inhibition of mSR.

Malonate is one of the most potent inhibitor published so far but its inhibition constant is high [84]. We thus decided to investigate whether the modifications of this compound on the α-carbon could lead to increase of inhibitory efficiency towards the enzyme. Our results suggest that malonate derivatives with small electronegative groups on the α-carbon possess higher binding affinity than compounds with bulky and more electropositive moieties (see Table 4, p. 24 and Figure 9, p. 47). It should be mentioned though that the effectivity with which the particular compound inhibits mSR does not correlate with the electonegativity and the size of the α-carbon substituent completely. For instance, in the initial compound screening, dichloromalonate was shown to be more potent mSR inhibitor than chloromalonate. Since 3D structure of hSR is already available, the computational experiments could probably help with explanation of this phenomenon.

In fact, further characterizations of selected inhibitors (see Table 5, p. 48) revealed that dichloromalonate is the only compound from the tested panel possessing higher affinity towards SR than malonate itself (K_i value 19 μM, see Figure 10, p. 49). Surprisingly, the K_i value for malonate determined in this study was 3-fold lower than the one previously published by our research group [84]. This difference was probably caused by slightly distinct preparations of SR. Indeed, even the K_m values for L-serine during racemisation reaction did not coincide completely (see above).

Despite the initial requirement that the compound must decrease the mSR activity by more than 98% to be considered for additional investigation, IC_{50} values of several malonate-based compounds with lower inhibitory potency were also determined (see Table 6, p. 50). The main purpose of these measurements was to collect data for ligands with different affinity towards mSR in order to compare the experimental results with theoretical modelling performed by Martin Lepšík and Dana Nachtigalová from IOCB. The outcome

of this study will not be discussed further since the computational experiments are still in the process of completion.

The last part of this project was focused on the characterization of 3-hydroxyglutamates as novel substrates of mSR. Initially, hydroxyglutamates and their derivatives were selected to be tested as potential inhibitors of mSR. This choice was deliberate since mentioned compounds are structural analogues of hydroxyaspartates and we thus wanted to investigate whether they can possess similar affinity to mSR. However, except of D-*threo*-3-hydroxyglutamate, none of the compounds decreased the activity of mSR significantly (see Figure 11, p. 51). On the other hand, it was observed that all stereoisomers of 3-hydroxyglutamate are degradated during the enzymatic reaction (see Figure 12, p. 52). Further exploration then revealed that these compounds are eliminated by mSR to α-ketoglutarate (see Figure 14, p. 54).

In fact, the finding that all 3-hydroxyglutamates are substrates of mSR during *β*-elimination was remarkable. Indeed, the elongation of the carbon scaffold of L-*erythro*-3-hydroxyaspartate for just one carbon results in transformation of mSR inhibitor to mSR substrate. Similarly, while D-*threo*-3-hydroxyaspartate does not show any affinity towards mSR [84], its 3-hydroxyglutamate analogue binds to the enzyme in order to be deaminated. It is not probably possible to experimentally explain these phenomenons. The computational analysis of mSR in the presence of 3-hydroxyglutamates would be thus very interesting.

To identify α-ketoglutarate in the reaction mixture, the published HPLC method for detection of pyruvate after L-serine elimination by mSR was employed [91]. This method uses a pre-column derivatization of the samples by 2,4-dinitrophenylhydrazine which is known to react with various 2-oxo acids including α-ketoglutarate, glyoxylate and pyruvate [112]. Indeed, the preliminary experiments suggested that the mentioned method can be used for α-ketoglutarate detection (see Figure 14, p. 54). However, the results obtained from subsequent Michaelis-Menten kinetics measurements seemed to be inconsistent. It is thus possible that the 2,4-dinitrophenylhydrazine derivatization is not quantitative. For this reason, we developed another method for α-ketoglutarate identification which is based on pre-column derivatization of the reaction mixtures by *o*-phenylenediamine [113-115].

Finally, kinetic constants of all 3-hydroxyglutamates were determined (see Table 8, p. 57). Surprisingly, L-*erythro*-3-hydroxyglutamate was observed to possess the highest k_{cat} identified for any SR substrate so far and D-*threo*-3-hydroxyglutamate was shown to have one of the lowest K_m determined to date (compare Table 8, p. 57 with Table 1, p. 12 and Table 2, p. 13). However, it is not plausible that the β-elimination of 3-hydroxyglutamates would be physiologically relevant since none of the compounds have been reported to be detected *in vivo*. On the other hand, the product of the reaction is not toxic and D-*threo*-3-hydroxyglutamate as the compound with highest effect on mSR racemisation activity could be thus possibly used as an alternative in regulation of the enzyme during NMDA receptor overactivation.

6. CONCLUSIONS

1. Recombinant mouse serine racemase was prepared using *E.coli* expression system and 4-step purification. The pure protein was enzymatically characterized.

2. 50 different compounds were tested for their inhibitory potency towards mSR. 4 malonate-based compounds as promising inhibitors and 4 stereoisomers of 3-hydroxyglutamate as novel substrates were identified.

3. The most potent malonate-based inhibitors as determined from the initial screening were characterized in terms of binding affinity and mechanism of action. Dichloromalonate was shown to be the most effective competitive inhibitor identified to date.

4. The kinetic constants of the novel substrates of mSR – 3-hydroxyglutamates – were determined. L-*erythro*-3-hydroxyglutamate was observed to possess the highest k_{cat} identified so far and D-*threo*-3-hydroxyglutamate was shown to have one of the lowest K_m determined to date.

7. ABBREVIATIONS

ADP, ATP	adenosine diphosphate, adenosine triphosphate
Aβ	amyloid β-peptide
ALS	amyotrophic lateral sclerosis
APS	ammonium persulfate
BSA	bovine serum albumin
CCD	charge-coupled device
CNS	central nervous system
CTP	cytidine triphosphate
Da	daltons
DAAO	D-amino acid oxidase
DMSO	dimethyl sulfoxide
DNA	deoxyribonucleic acid
DNPH	dinitrophenylhydrazine
DTT	1,4-dithiothreitol
E.coli	*Escherichia coli*
EDTA	ethylenediaminetetraacetic acid
EST	expressed sequence tag
FAD	flavin adenine dinucleotide
FDAA	1-fluoro-2-4-dinitrophenyl-5-L-alanine amide (Marfey's Reagent)
GCS	glycine cleavage system
GRIP	glutamate receptor interacting protein
GTP	guanosine triphosphate
HEPES	4-(2-hydroxyethyl)-1-piperazineethanesulfonic acid
HPLC	high-performance liquid chromatography
hSR	human serine racemase
IOCB	Institute of Organic Chemistry and Biochemistry
kDa	1000 Daltons
LB	Luria-Bertani Broth
LS	L-serine
LTP	long-term potentiation
mRNA	messenger RNA

mSR	mouse serin racemase
NCBI	National Center of Biotechnology Information
NMDA	N-methyl-D-aspartate
OD	optical density
PAGE	polyacrylamide gel electrophoresis
PDB	Protein Data Bank
PICK1	protein interacting with kinase C
PLP	pyridoxal-5’-phosphate
RNA	ribonucleic acid
rSR	rat serine racemase
SDS	sodium dodecyl sulfate
SR	serine racemase
TBA	tetrabutylammonium
TCEP	triscarboxyethylphosphine
TEA	triethanolamine
TEMED	tetramethylethylendiamine
Tris	tris(hydroxymethyl)aminomethane
UTP	uridine triphosphate

8. REFERENCES

1. Corrigan, J.J. D-amino acids in animals. *Science* **164**, 142-149 (1969).

2. Hoeprich, P.D. Alanine: Cycloserine Antagonism. Vi. Demonstration of D-Alanine in the Serum of Guinea Pigs and Mice. *J Biol Chem* **240**, 1654-1660 (1965).

3. Dunlop, D.S., Neidle, A., McHale, D., Dunlop, D.M. & Lajtha, A. The presence of free D-aspartic acid in rodents and man. *Biochem Biophys Res Commun* **141**, 27-32 (1986).

4. Man, E.H., Fisher, G.H., Payan, I.L., Cadilla-Perezrios, R., Garcia, N.M., Chemburkar, R., Arends, G. & Frey, W.H., 2nd. D-aspartate in human brain. *J Neurochem* **48**, 510-515 (1987).

5. Neidle, A. & Dunlop, D.S. Developmental changes in free D-aspartic acid in the chicken embryo and in the neonatal rat. *Life Sci* **46**, 1517-1522 (1990).

6. Hashimoto, A., Nishikawa, T., Hayashi, T., Fujii, N., Harada, K., Oka, T. & Takahashi, K. The presence of free D-serine in rat brain. *FEBS Lett* **296**, 33-36 (1992).

7. Hashimoto, A., Kumashiro, S., Nishikawa, T., Oka, T., Takahashi, K., Mito, T., Takashima, S., Doi, N., Mizutani, Y., Yamazaki, T. & et al. Embryonic development and postnatal changes in free D-aspartate and D-serine in the human prefrontal cortex. *J Neurochem* **61**, 348-351 (1993).

8. Kleckner, N.W. & Dingledine, R. Requirement for glycine in activation of NMDA-receptors expressed in Xenopus oocytes. *Science* **241**, 835-837 (1988).

9. Oldendorf, W.H. Stereospecificity of blood-brain barrier permeability to amino acids. *Am J Physiol* **224**, 967-969 (1973).

10. Dunlop, D.S. & Neidle, A. The origin and turnover of D-serine in brain. *Biochem Biophys Res Commun* **235**, 26-30 (1997).

11. Takahashi, K., Hayashi, F. & Nishikawa, T. In vivo evidence for the link between L- and D-serine metabolism in rat cerebral cortex. *J Neurochem* **69**, 1286-1290 (1997).

12. Wolosker, H., Sheth, K.N., Takahashi, M., Mothet, J.P., Brady, R.O., Jr., Ferris, C.D. & Snyder, S.H. Purification of serine racemase: biosynthesis of the neuromodulator D-serine. *Proc Natl Acad Sci U S A* **96**, 721-725 (1999).

13. Billard, J.M. D-Amino acids in brain neurotransmission and synaptic plasticity. *Amino Acids* **43**, 1851-1860 (2012).

14. Fuchs, S.A., Berger, R. & de Koning, T.J. D-serine: the right or wrong isoform? *Brain Res* **1401**, 104-117 (2011).

15. Nishikawa, T. Analysis of free D-serine in mammals and its biological relevance. *J Chromatogr B Analyt Technol Biomed Life Sci* **879**, 3169-3183 (2011).

16. Ohide, H., Miyoshi, Y., Maruyama, R., Hamase, K. & Konno, R. D-Amino acid metabolism in mammals: biosynthesis, degradation and analytical aspects of the metabolic study. *J Chromatogr B Analyt Technol Biomed Life Sci* **879**, 3162-3168 (2011).

17. Danysz, W. & Parsons, C.G. Glycine and N-methyl-D-aspartate receptors: physiological significance and possible therapeutic applications. *Pharmacol Rev* **50**, 597-664 (1998).

18. Dingledine, R., Borges, K., Bowie, D. & Traynelis, S.F. The glutamate receptor ion channels. *Pharmacol Rev* **51**, 7-61 (1999).

19. Kandel, E., Schwartz, J., Jessell, T., Siegelbaum, S. & Hudspeth, A.J. Principles of Neural Science, Fifth Edition. *McGraw-Hill Education*, (2012).

20. Wroblewski, J.T., Fadda, E., Mazzetta, J., Lazarewicz, J.W. & Costa, E. Glycine and D-serine act as positive modulators of signal transduction at N-methyl-D-aspartate sensitive glutamate receptors in cultured cerebellar granule cells. *Neuropharmacology* **28**, 447-452 (1989).

21. McBain, C.J., Kleckner, N.W., Wyrick, S. & Dingledine, R. Structural requirements for activation of the glycine coagonist site of N-methyl-D-aspartate receptors expressed in Xenopus oocytes. *Mol Pharmacol* **36**, 556-565 (1989).

22. Kouparis, L. Anaesthesia UK: NMDA receptor online [online]. 2005 [cited 21.3.2013]. Available at http://www.frca.co.uk/images/NMDA.jpg.

23. Hashimoto, A., Nishikawa, T., Oka, T. & Takahashi, K. Endogenous D-serine in rat brain: N-methyl-D-aspartate receptor-related distribution and aging. *J Neurochem* **60**, 783-786 (1993).

24. Schell, M.J., Brady, R.O., Jr., Molliver, M.E. & Snyder, S.H. D-serine as a neuromodulator: regional and developmental localizations in rat brain glia resemble NMDA receptors. *J Neurosci* **17**, 1604-1615 (1997).

25. Matsui, T., Sekiguchi, M., Hashimoto, A., Tomita, U., Nishikawa, T. & Wada, K. Functional comparison of D-serine and glycine in rodents: the effect on cloned NMDA receptors and the extracellular concentration. *J Neurochem* **65**, 454-458 (1995).

26. Furukawa, H. & Gouaux, E. Mechanisms of activation, inhibition and specificity: crystal structures of the NMDA receptor NR1 ligand-binding core. *EMBO J* **22**, 2873-2885 (2003).

27. Stevens, E.R., Gustafson, E.C. & Miller, R.F. Glycine transport accounts for the differential role of glycine vs. D-serine at NMDA receptor coagonist sites in the salamander retina. *Eur J Neurosci* **31**, 808-816 (2010).

28. Mothet, J.P., Parent, A.T., Wolosker, H., Brady, R.O., Jr., Linden, D.J., Ferris, C.D., Rogawski, M.A. & Snyder, S.H. D-serine is an endogenous ligand for the glycine site of the N-methyl-D-aspartate receptor. *Proc Natl Acad Sci U S A* **97**, 4926-4931 (2000).

29. Stevens, E.R., Esguerra, M., Kim, P.M., Newman, E.A., Snyder, S.H., Zahs, K.R. & Miller, R.F. D-serine and serine racemase are present in the vertebrate retina and contribute to the physiological activation of NMDA receptors. *Proc Natl Acad Sci U S A* **100**, 6789-6794 (2003).

30. Shleper, M., Kartvelishvily, E. & Wolosker, H. D-serine is the dominant endogenous coagonist for NMDA receptor neurotoxicity in organotypic hippocampal slices. *J Neurosci* **25**, 9413-9417 (2005).

31. Kartvelishvily, E., Shleper, M., Balan, L., Dumin, E. & Wolosker, H. Neuron-derived D-serine release provides a novel means to activate N-methyl-D-aspartate receptors. *J Biol Chem* **281**, 14151-14162 (2006).

32. Panatier, A., Theodosis, D.T., Mothet, J.P., Touquet, B., Pollegioni, L., Poulain, D.A. & Oliet, S.H. Glia-derived D-serine controls NMDA receptor activity and synaptic memory. *Cell* **125**, 775-784 (2006).

33. Gustafson, E.C., Stevens, E.R., Wolosker, H. & Miller, R.F. Endogenous D-serine contributes to NMDA-receptor-mediated light-evoked responses in the vertebrate retina. *J Neurophysiol* **98**, 122-130 (2007).

34. Mori, H. & Inoue, R. Serine racemase knockout mice. *Chem Biodivers* **7**, 1573-1578 (2010).

35. Huang, X., Kong, H., Tang, M., Lu, M., Ding, J.H. & Hu, G. D-Serine regulates proliferation and neuronal differentiation of neural stem cells from postnatal mouse forebrain. *CNS Neurosci Ther* **18**, 4-13 (2012).

36. Henneberger, C., Papouin, T., Oliet, S.H. & Rusakov, D.A. Long-term potentiation depends on release of D-serine from astrocytes. *Nature* **463**, 232-236 (2010).

37. Kalia, L.V., Kalia, S.K. & Salter, M.W. NMDA receptors in clinical neurology: excitatory times ahead. *Lancet Neurol* **7**, 742-755 (2008).

38. Fuchs, S.A., Berger, R., Klomp, L.W. & de Koning, T.J. D-amino acids in the central nervous system in health and disease. *Mol Genet Metab* **85**, 168-180 (2005).

39. Wolosker, H., Dumin, E., Balan, L. & Foltyn, V.N. D-amino acids in the brain: D-serine in neurotransmission and neurodegeneration. *FEBS J* **275**, 3514-3526 (2008).

40. Nagata, Y., Masui, R. & Akino, T. The presence of free D-serine, D-alanine and D-proline in human plasma. *Experientia* **48**, 986-988 (1992).

41. Rotgans, J., Wodarz, R., Schoknecht, W. & Drysch, K. The determination of amino-acid enantiomers in human saliva with Chirasil-Val. *Arch Oral Biol* **28**, 1121-1124 (1983).

42. Bruckner, H., Haasmann, S. & Friedrich, A. Quantification of D-Amino Acids in Human Urine Using Gc-Ms and Hplc. *Amino Acids* **6**, 205-211 (1994).

43. Ghasemi-Kasman, M., Dehpour, A.R. & Mani, A.R. D-serine modulates non-adrenergic non-cholinergic contraction of lower esophageal sphincter in rats. *Eur J Pharmacol* **696**, 155-160 (2012).

44. Ghasemi, M., Rezania, F., Lewin, J., Moore, K.P. & Mani, A.R. d-Serine modulates neurogenic relaxation in rat corpus cavernosum. *Biochem Pharmacol* **79**, 1791-1796 (2010).

45. Takarada, T., Takahata, Y., Iemata, M., Hinoi, E., Uno, K., Hirai, T., Yamamoto, T. & Yoneda, Y. Interference with cellular differentiation by D-serine through antagonism at N-methyl-D-aspartate receptors composed of NR1 and NR3A subunits in chondrocytes. *J Cell Physiol* **220**, 756-764 (2009).

46. Takarada, T., Takarada-Iemata, M., Takahata, Y., Yamada, D., Yamamoto, T., Nakamura, Y., Hinoi, E. & Yoneda, Y. Osteoclastogenesis is negatively regulated by D-serine produced by osteoblasts. *J Cell Physiol* **227**, 3477-3487 (2012).

47. Bauer, D., Hamacher, K., Broer, S., Pauleit, D., Palm, C., Zilles, K., Coenen, H.H. & Langen, K.J. Preferred stereoselective brain uptake of d-serine--a modulator of glutamatergic neurotransmission. *Nucl Med Biol* **32**, 793-797 (2005).

48. Iwama, H., Takahashi, K., Kure, S., Hayashi, F., Narisawa, K., Tada, K., Mizoguchi, M., Takashima, S., Tomita, U. & Nishikawa, T. Depletion of cerebral D-serine in non-ketotic hyperglycinemia: possible involvement of glycine cleavage system in control of endogenous D-serine. *Biochem Biophys Res Commun* **231**, 793-796 (1997).

49. Wood, P.L., Hawkinson, J.E. & Goodnough, D.B. Formation of D-serine from L-phosphoserine in brain synaptosomes. *J Neurochem* **67**, 1485-1490 (1996).

50. Kikuchi, G., Motokawa, Y., Yoshida, T. & Hiraga, K. Glycine cleavage system: reaction mechanism, physiological significance, and hyperglycinemia. *Proc Jpn Acad Ser B Phys Biol Sci* **84**, 246-263 (2008).

51. Goodnough, D.B., Lutz, M.P. & Wood, P.L. Separation and quantification of D- and L-phosphoserine in rat brain using N alpha-(2,4-dinitro-5-fluorophenyl)-L-alaninamide (Marfey's reagent) by high-performance liquid chromatography with ultraviolet detection. *J Chromatogr B Biomed Appl* **672**, 290-294 (1995).

52. Park, H.K., Shishido, Y., Ichise-Shishido, S., Kawazoe, T., Ono, K., Iwana, S., Tomita, Y., Yorita, K., Sakai, T. & Fukui, K. Potential role for astroglial D-amino acid oxidase in extracellular D-serine metabolism and cytotoxicity. *J Biochem* **139**, 295-304 (2006).

53. Molla, G., Sacchi, S., Bernasconi, M., Pilone, M.S., Fukui, K. & Polegioni, L. Characterization of human D-amino acid oxidase. *FEBS Lett* **580**, 2358-2364 (2006).

54. Pollegioni, L. & Sacchi, S. Metabolism of the neuromodulator D-serine. *Cell Mol Life Sci* **67**, 2387-2404 (2010).

55. Yamanaka, M., Miyoshi, Y., Ohide, H., Hamase, K. & Konno, R. D-Amino acids in the brain and mutant rodents lacking D-amino-acid oxidase activity. *Amino Acids* **43**, 1811-1821 (2012).

56. Foltyn, V.N., Bendikov, I., De Miranda, J., Panizzutti, R., Dumin, E., Shleper, M., Li, P., Toney, M.D., Kartvelishvily, E. & Wolosker, H. Serine racemase modulates intracellular D-serine levels through an alpha,beta-elimination activity. *J Biol Chem* **280**, 1754-1763 (2005).

57. Jirásková, J. Mammalian Serine Racemase as a Pharmaceutical Target: Dissertation, Faculty of Science, Charles University in Prague (2010).

58. Hoffman, H.E. Characterization of recombinant human serine racemase: Dissertation, Faculty of Science, Charles University in Prague (2010).

59. NCBI. EST Profile – Hs.461954 [online]. 2013 [cited 5.5.2013]. Available at http://www.ncbi.nlm.nih.gov/UniGene/ESTProfileViewer.cgi?uglist=Hs.461954.

60. Xia, M., Liu, Y., Figueroa, D.J., Chiu, C.S., Wei, N., Lawlor, A.M., Lu, P., Sur, C., Koblan, K.S. & Connolly, T.M. Characterization and localization of a human serine racemase. *Brain Res Mol Brain Res* **125**, 96-104 (2004).

61. Wang, L.Z. & Zhu, X.Z. Spatiotemporal relationships among D-serine, serine racemase, and D-amino acid oxidase during mouse postnatal development. *Acta Pharmacol Sin* **24**, 965-974 (2003).

62. Wu, S., Barger, S.W. & Sims, T.J. Schwann cell and epineural fibroblast expression of serine racemase. *Brain Res* **1020**, 161-166 (2004).

63. Dun, Y., Duplantier, J., Roon, P., Martin, P.M., Ganapathy, V. & Smith, S.B. Serine racemase expression and D-serine content are developmentally regulated in neuronal ganglion cells of the retina. *J Neurochem* **104**, 970-978 (2008).

64. Dememes, D., Mothet, J.P. & Nicolas, M.T. Cellular distribution of D-serine, serine racemase and D-amino acid oxidase in the rat vestibular sensory epithelia. *Neuroscience* **137**, 991-997 (2006).

65. Wolosker, H., Blackshaw, S. & Snyder, S.H. Serine racemase: a glial enzyme synthesizing D-serine to regulate glutamate-N-methyl-D-aspartate neurotransmission. *Proc Natl Acad Sci U S A* **96**, 13409-13414 (1999).

66. Yasuda, E., Ma, N. & Semba, R. Immunohistochemical evidences for localization and production of D-serine in some neurons in the rat brain. *Neurosci Lett* **299**, 162-164 (2001).

67. Ding, X., Ma, N., Nagahama, M., Yamada, K. & Semba, R. Localization of D-serine and serine racemase in neurons and neuroglias in mouse brain. *Neurol Sci* **32**, 263-267 (2011).

68. Yoshikawa, M., Takayasu, N., Hashimoto, A., Sato, Y., Tamaki, R., Tsukamoto, H., Kobayashi, H. & Noda, S. The serine racemase mRNA is predominantly expressed in rat brain neurons. *Arch Histol Cytol* **70**, 127-134 (2007).

69. Miya, K., Inoue, R., Takata, Y., Abe, M., Natsume, R., Sakimura, K., Hongou, K., Miyawaki, T. & Mori, H. Serine racemase is predominantly localized in neurons in mouse brain. *J Comp Neurol* **510**, 641-654 (2008).

70. Balan, L., Foltyn, V.N., Zehl, M., Dumin, E., Dikopoltsev, E., Knoh, D., Ohno, Y., Kihara, A., Jensen, O.N., Radzishevsky, I.S. & Wolosker, H. Feedback inactivation of D-serine synthesis by NMDA receptor-elicited translocation of serine racemase to the membrane. *Proc Natl Acad Sci U S A* **106**, 7589-7594 (2009).

71. Basu, A.C., Tsai, G.E., Ma, C.L., Ehmsen, J.T., Mustafa, A.K., Han, L., Jiang, Z.I., Benneyworth, M.A., Froimowitz, M.P., Lange, N., Snyder, S.H., Bergeron, R. & Coyle, J.T. Targeted disruption of serine racemase affects glutamatergic neurotransmission and behavior. *Mol Psychiatry* **14**, 719-727 (2009).

72. Inoue, R., Hashimoto, K., Harai, T. & Mori, H. NMDA- and beta-amyloid1-42-induced neurotoxicity is attenuated in serine racemase knock-out mice. *J Neurosci* **28**, 14486-14491 (2008).

73. Mustafa, A.K., Ahmad, A.S., Zeynalov, E., Gazi, S.K., Sikka, G., Ehmsen, J.T., Barrow, R.K., Coyle, J.T., Snyder, S.H. & Dore, S. Serine racemase deletion protects against cerebral ischemia and excitotoxicity. *J Neurosci* **30**, 1413-1416 (2010).

74. DeVito, L.M., Balu, D.T., Kanter, B.R., Lykken, C., Basu, A.C., Coyle, J.T. & Eichenbaum, H. Serine racemase deletion disrupts memory for order and alters cortical dendritic morphology. *Genes Brain Behav* **10**, 210-222 (2011).

75. Dunlop, D.S. & Neidle, A. Regulation of serine racemase activity by amino acids. *Brain Res Mol Brain Res* **133**, 208-214 (2005).

76. Wolosker, H. & Mori, H. Serine racemase: an unconventional enzyme for an unconventional transmitter. *Amino Acids* **43**, 1895-1904 (2012).

77. Hashimoto, K., Fukushima, T., Shimizu, E., Komatsu, N., Watanabe, H., Shinoda, N., Nakazato, M., Kumakiri, C., Okada, S., Hasegawa, H., Imai, K. & Iyo, M. Decreased serum levels of D-serine in patients with schizophrenia: evidence in support of the N-methyl-D-aspartate receptor hypofunction hypothesis of schizophrenia. *Arch Gen Psychiatry* **60**, 572-576 (2003).

78. Bendikov, I., Nadri, C., Amar, S., Panizzutti, R., De Miranda, J., Wolosker, H. & Agam, G. A CSF and postmortem brain study of D-serine metabolic parameters in schizophrenia. *Schizophr Res* **90**, 41-51 (2007).

79. Wu, S.Z., Bodles, A.M., Porter, M.M., Griffin, W.S., Basile, A.S. & Barger, S.W. Induction of serine racemase expression and D-serine release from microglia by amyloid beta-peptide. *J Neuroinflammation* **1**, 2 (2004).

80. Sasabe, J., Chiba, T., Yamada, M., Okamoto, K., Nishimoto, I., Matsuoka, M. & Aiso, S. D-serine is a key determinant of glutamate toxicity in amyotrophic lateral sclerosis. *EMBO J* **26**, 4149-4159 (2007).

81. Thompson, M., Marecki, J.C., Marinesco, S., Labrie, V., Roder, J.C., Barger, S.W. & Crow, J.P. Paradoxical roles of serine racemase and D-serine in the G93A mSOD1 mouse model of amyotrophic lateral sclerosis. *J Neurochem* **120**, 598-610 (2012).

82. Ryu, H.J., Kim, J.E., Yeo, S.I., Kim, D.S., Kwon, O.S., Choi, S.Y. & Kang, T.C. Potential roles of D-serine and serine racemase in experimental temporal lobe epilepsy. *J Neurosci Res* **88**, 2469-2482 (2010).

83. Harai, T., Inoue, R., Fujita, Y., Tanaka, A., Horio, M., Hashimoto, K., Hongou, K., Miyawaki, T. & Mori, H. Decreased susceptibility to seizures induced by pentylenetetrazole in serine racemase knockout mice. *Epilepsy Res* **102**, 180-187 (2012).

84. Strisovsky, K., Jiraskova, J., Mikulova, A., Rulisek, L. & Konvalinka, J. Dual substrate and reaction specificity in mouse serine racemase: identification of high-affinity dicarboxylate substrate and inhibitors and analysis of the beta-eliminase activity. *Biochemistry* **44**, 13091-13100 (2005).

85. Hoffman, H.E., Jiraskova, J., Ingr, M., Zvelebil, M. & Konvalinka, J. Recombinant human serine racemase: enzymologic characterization and comparison with its mouse ortholog. *Protein Expr Purif* **63**, 62-67 (2009).

86. Krug, A.W., Volker, K., Dantzler, W.H. & Silbernagl, S. Why is D-serine nephrotoxic and alpha-aminoisobutyric acid protective? *Am J Physiol Renal Physiol* **293**, F382-390 (2007).

87. De Miranda, J., Panizzutti, R., Foltyn, V.N. & Wolosker, H. Cofactors of serine racemase that physiologically stimulate the synthesis of the N-methyl-D-aspartate (NMDA) receptor coagonist D-serine. *Proc Natl Acad Sci U S A* **99**, 14542-14547 (2002).

88. Strisovsky, K., Jiraskova, J., Barinka, C., Majer, P., Rojas, C., Slusher, B.S. & Konvalinka, J. Mouse brain serine racemase catalyzes specific elimination of L-serine to pyruvate. *FEBS Lett* **535**, 44-48 (2003).

89. Jiraskova-Vanickova, J., Ettrich, R., Vorlova, B., Hoffman, H.E., Lepsik, M., Jansa, P. & Konvalinka, J. Inhibition of human serine racemase, an emerging target for medicinal chemistry. *Curr Drug Targets* **12**, 1037-1055 (2011).

90. Cook, S.P., Galve-Roperh, I., Martinez del Pozo, A. & Rodriguez-Crespo, I. Direct calcium binding results in activation of brain serine racemase. *J Biol Chem* **277**, 27782-27792 (2002).

91. Neidle, A. & Dunlop, D.S. Allosteric regulation of mouse brain serine racemase. *Neurochem Res* **27**, 1719-1724 (2002).

92. Hoffman, H., Jiraskova, J., Zvelebil, M. & Konvalinka, J. Random mutagenesis of human serine racemase reveals residues important for the enzymatic activity. *Collect. Czech. Chem. Commun* **75**, 59-79 (2010).

93. Mustafa, A.K., Kumar, M., Selvakumar, B., Ho, G.P., Ehmsen, J.T., Barrow, R.K., Amzel, L.M. & Snyder, S.H. Nitric oxide S-nitrosylates serine racemase, mediating feedback inhibition of D-serine formation. *Proc Natl Acad Sci U S A* **104**, 2950-2955 (2007).

94. Lopez-Mirabal, H.R. & Winther, J.R. Redox characteristics of the eukaryotic cytosol. *Biochim Biophys Acta* **1783**, 629-640 (2008).

95. Dumin, E., Bendikov, I., Foltyn, V.N., Misumi, Y., Ikehara, Y., Kartvelishvily, E. & Wolosker, H. Modulation of D-serine levels via ubiquitin-dependent proteasomal degradation of serine racemase. *J Biol Chem* **281**, 20291-20302 (2006).

96. Baumgart, F. & Rodriguez-Crespo, I. D-amino acids in the brain: the biochemistry of brain serine racemase. *FEBS J* **275**, 3538-3545 (2008).

97. Kim, P.M., Aizawa, H., Kim, P.S., Huang, A.S., Wickramasinghe, S.R., Kashani, A.H., Barrow, R.K., Huganir, R.L., Ghosh, A. & Snyder, S.H. Serine racemase: activation by glutamate neurotransmission via glutamate receptor interacting protein and mediation of neuronal migration. *Proc Natl Acad Sci U S A* **102**, 2105-2110 (2005).

98. Baumgart, F., Mancheno, J.M. & Rodriguez-Crespo, I. Insights into the activation of brain serine racemase by the multi-PDZ domain glutamate receptor interacting protein, divalent cations and ATP. *FEBS J* **274**, 4561-4571 (2007).

99. Hikida, T., Mustafa, A.K., Maeda, K., Fujii, K., Barrow, R.K., Saleh, M., Huganir, R.L., Snyder, S.H., Hashimoto, K. & Sawa, A. Modulation of D-serine levels in brains of mice lacking PICK1. *Biol Psychiatry* **63**, 997-1000 (2008).

100. Larkin, M.A., Blackshields, G., Brown, N.P., Chenna, R., McGettigan, P.A., McWilliam, H., Valentin, F., Wallace, I.M., Wilm, A., Lopez, R., Thompson, J.D., Gibson, T.J. & Higgins, D.G. Clustal W and Clustal X version 2.0. *Bioinformatics* **23**, 2947-2948 (2007).

101. Smith, M.A., Mack, V., Ebneth, A., Moraes, I., Felicetti, B., Wood, M., Schonfeld, D., Mather, O., Cesura, A. & Barker, J. The structure of mamalian serine racemase: Evidence for conformational changes upon inhibitor binding. *J Biol Chem* (2010).

102. DeLano, W.L. The PyMOL Molecular Graphics System. *DeLano Scientific*, San Carlos, USA (2002).

103. Hoffman, H.E., Jiraskova, J., Cigler, P., Sanda, M., Schraml, J. & Konvalinka, J. Hydroxamic acids as a novel family of serine racemase inhibitors: mechanistic analysis reveals different modes of interaction with the pyridoxal-5'-phosphate cofactor. *J Med Chem* **52**, 6032-6041 (2009).

104. Dixon, S.M., Li, P., Liu, R., Wolosker, H., Lam, K.S., Kurth, M.J. & Toney, M.D. Slow-binding human serine racemase inhibitors from high-throughput screening of combinatorial libraries. *J Med Chem* **49**, 2388-2397 (2006).

105. Panizzutti, R., De Miranda, J., Ribeiro, C.S., Engelender, S. & Wolosker, H. A new strategy to decrease N-methyl-D-aspartate (NMDA) receptor coactivation: inhibition of D-serine synthesis by converting serine racemase into an eliminase. *Proc Natl Acad Sci U S A* **98**, 5294-5299 (2001).

106. Laurido, C., Hernandez, A., Pelissier, T. & Constandil, L. Antinociceptive effect of rat D-serine racemase inhibitors, L-serine-O-sulfate, and L-erythro-3-hydroxyaspartate in an arthritic pain model. *ScientificWorldJournal* **2012**, 279147 (2012).

107. Vorlová, B. Studium exprese serinracemasy v CNS pacientů postižených epilepsií: Bakalářská práce, Přírodovědecká Fakulta, Univerzita Karlova v Praze (2010).

108. Bradford, M.M. A rapid and sensitive method for the quantitation of microgram quantities of protein utilizing the principle of protein-dye binding. *Anal Biochem* **72**, 248-254 (1976).

109. Leatherbarrow, R.J. GraFit Version 7. *Erithacus Software Ltd.*, Horley, UK (2009).

110. Lineweaver, H. & Burk, D. The Determination of Enzyme Dissociation Constants. *J Am Chem Soc* **56**(1934).

111. Wang, W. & Barger, S.W. Roles of quaternary structure and cysteine residues in the activity of human serine racemase. *BMC Biochem* **12**, 63 (2011).

112. Lange, M. & Malyusz, M. Fast method for the simultaneous determination of 2-oxo acids in biological fluids by high-performance liquid chromatography. *J Chromatogr B Biomed Appl* **662**, 97-102 (1994).

113. McNeill, L.A., Bethge, L., Hewitson, K.S. & Schofield, C.J. A fluorescence-based assay for 2-oxoglutarate-dependent oxygenases. *Anal Biochem* **336**, 125-131 (2005).

114. Muhling, J., Fuchs, M., Campos, M.E., Gonter, J., Engel, J.M., Sablotzki, A., Menges, T., Weiss, S., Dehne, M.G., Krull, M. & Hempelmann, G. Quantitative determination of free intracellular alpha-keto acids in neutrophils. *J Chromatogr B Analyt Technol Biomed Life Sci* **789**, 383-392 (2003).

115. Singh, B.K., Szamosi, I. & Shaner, D. A high-performance liquid chromatography assay for threonine/serine dehydratase. *Anal Biochem* **208**, 260-263 (1993).

Svoluji k zapůjčení této práce pro studijní účely a prosím, aby byla řádně vedena evidence zapůjčovatelů.

Jméno a příjmení s adresou	Číslo OP	Datum vypůjčení	Poznámka